Chinese Chemical Letters 36 (2025) 110600

Contents lists available at ScienceDirect

Chinese Chemical Letters

journal homepage: www.elsevier.com/locate/cclet

Recent advances in supramolecular luminescent materials based on macrocyclic arenes

Yu-Jie Long[a,b], Xiao-Ni Han[a], Ying Han[a,*], Chuan-Feng Chen[a,b,*]

[a] Beijing National Laboratory for Molecular Sciences, CAS Key Laboratory of Molecular Recognition and Function, Institute of Chemistry, Chinese Academy of Sciences, Beijing 100190, China
[b] University of Chinese Academy of Sciences, Beijing 100049, China

ARTICLE INFO

Article history:
Received 3 September 2024
Revised 21 October 2024
Accepted 30 October 2024
Available online 2 November 2024

Keywords:
Supramolecular luminescent materials
Macrocyclic arenes
Supramolecular assemblies
Host-guest complexes
Supramolecular polymers
Supramolecular nanoparticles

ABSTRACT

Supramolecular luminescent materials (SLMs) exhibit exceptional luminescence properties and the ability to be intelligently regulated through diverse assembly approaches, making them highly attractive in the field of luminescent materials. In recent years, the novel macrocyclic arenes characterized by unique electron-rich structures, ease of derivatization, tunable conformations and even inherent luminescence properties afford much opportunities to create such dynamic smart luminescent materials. The incorporation of macrocyclic arenes into SLMs leads to simple preparation process, diverse photophysical phenomena and sophisticated regulatory mechanisms, which is also currently one of the most frontier and hot topics in macrocyclic and supramolecular chemistry and even luminescent materials. In this review, the research advances in construction and applications of SLMs based on macrocyclic arenes in the last several years will be presented from the different assembly strategies, including host-guest complexes, supramolecular polymers, nanoparticles, and other assemblies. Moreover, some insights into future directions for this research area will also be offered.

1. Introduction

Supramolecular luminescent materials (SLMs) have aroused great interests in recent years due to their simple synthesis, unique luminescent properties, and dynamically reversible and versatile function features [1]. Utilizing supramolecular strategies into different photophysical processes, such as fluorescence [2], thermally activated delayed fluorescence (TADF) [3], room-temperature phosphorescence (RTP) [4], energy transfer and electron transfer processes [5], have wide applications in bioimaging [6,7], optical sensors [8,9], molecular switches [10,11], anti-counterfeiting materials [12,13] and organic light-emitting diodes (OLEDs) [14]. Due to the existence of dynamic and reversible noncovalent interactions, such as hydrogen bonding, C–H···π, π-π stacking, hydrophobic effects, electrostatic effects, charge transfer (CT) interactions and so on [15], SLMs exhibit outstanding luminescence properties and intelligent regulation through diverse assembly approaches. Additionally, the supramolecular strategies also offer advantages in synthesis routes over traditional covalent synthesis methods, which lead to the reduced synthesis costs and simpler preparation processes. Therefore, SLMs have become one of the most frontier and hot topics in supramolecular chemistry and materials chemistry.

Among various SLMs, those ones constructed through the host-guest interaction of macrocycles have attracted considerable attention in recent years owing to the ability of macrocyclic intrinsic cavities to effectively dynamic encapsulate guest molecules, leading to the formation of supramolecular luminescent materials. Moreover, the flexible and tunable conformation and multiple noncovalent complexation sites of the macrocyclic hosts also afford a new opportunity to create such dynamic smart luminescent materials.

Macrocyclic arenes are a type of macrocyclic compound with rich-electron aromatic rings bridged by sp^3 carbon atoms [16,17]. In recent years, an increasing number of novel macrocyclic arenes have been reported [18–21]. They have shown wide applications in diverse research fields including molecular machines [22,23], molecular recognition and assemblies [24–26], and biomedical science [27]. With the rapid development of macrocyclic and supramolecular chemistry, macrocyclic arenes with novel structures have emerged as one of the most significant and extensively studied classes of synthetic macrocyclic hosts [19]. In comparison to other macrocyclic hosts, macrocyclic arenes have flexible and definite conformation, unique optical features, and multiple binding sites. Integration of these macrocyclic arenes into supramolec-

* Corresponding authors.
E-mail addresses: hanying463@iccas.ac.cn (Y. Han), cchen@iccas.ac.cn (C.-F. Chen).

https://doi.org/10.1016/j.cclet.2024.110600
1001-8417/

ular luminescent materials can promise diverse photophysical phenomena and regulatory mechanisms, thereby offering opportunities for deeper exploration in this field [28–31].

In recent years, more and more novel supramolecular luminescent materials based on macrocyclic arenes have been constructed and found their wide applications in molecular recognition and sensing, information encryption, bioimaging and so on. Therefore, it is urgent to systematically and comprehensively summarize the recent advances in the preparation strategies, properties, and applications of the supramolecular luminescent materials based on macrocyclic arenes. In this review, we will present the research progress of SLMs based on macrocyclic arenes in the last several years. Consequently, we will introduce these SLMs from the perspective of the supramolecular assembly strategies, including host-guest complexes, supramolecular polymers, nanoparticles and other assemblies. Moreover, we will also offer some insights into future directions for this research area. We believe this review focusing on SLMs based on the macrocyclic arenes will promote the development of macrocycle and supramolecular chemistry and also provide some guidance toward the design and construction of smart supramolecular luminescent materials.

2. Host-guest complexes

Macrocyclic arenes possess well-defined cavities and multiple binding sites, which allow them to form host-guest complexes with a wide variety of guests through noncovalent interactions. In these complexes, the cavities of the macrocyclic arenes often restrict the free rotation of the guest molecules or alter their aggregation states, thereby influencing the photophysical properties of the complexes.

In 2019, Yang's group obtained a host-guest complex **G1⊂1** [32]. The host-guest complexation between **1** and **G1** restricted the intramolecular rotation of **G1**, reducing non-radiative relaxation. As a result, **G1⊂1** (Fig. 1) exhibited strong blue emission with a significantly higher quantum yield and a longer fluorescence lifetime compared to free **G1**. Additionally, the fluorescence of **G1⊂1** could be quenched by the ligand interaction of **1** with Fe^{3+}, which was highly selective and sensitive. They also synthesized **G2⊂2** (Fig. 1) [33]. The fluorescence of **G2⊂2** could be quenched by Hg^{2+}, and the formation of **G2⊂2@Hg^{2+}** could also be used for the sensitive recognition of L-cysteine. This luminescent material was expected to wide applications in fluorescence sensing, cell imaging and visualized monitoring.

In host-guest complexes, macrocyclic arenes can also alter the stacking modes of the guest molecules, thereby preventing the aggregation-induced quenching (ACQ) effect or changing the emission state of the guests. In 2022, Yang's group [34] synthesized a methoxy pillar[5]arene (P5) dimer **3** bridged by a 2,3,6,7-tetramethoxy-9,10-di-*p*-tolylanthracene linker (Fig. 2b). The P5 units prevented intermolecular π-π stacking, resulting in **3**

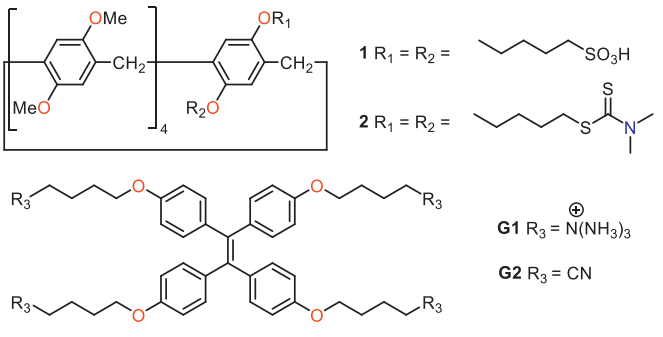

Fig. 1. Chemical structures of **1**, **2**, **G1** and **G2**.

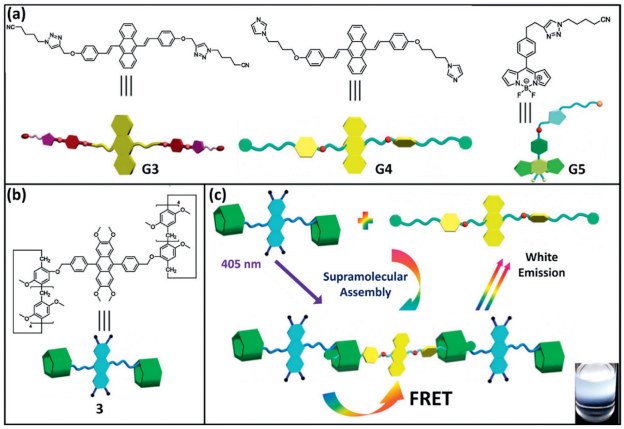

Fig. 2. Chemical structures of (a) **G3**, **G4**, **G5** and (b) **3**. (c) Schematic illustration of the supramolecular assembly based on **3** and **G4**, and the white-light emission adjusted by the host-guest interactions. Reproduced with permission [34]. Copyright 2019, Wiley Publisher.

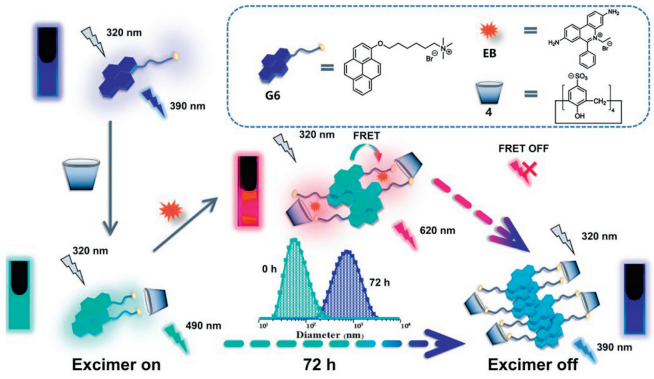

Fig. 3. Chemical structures of **4** and **G6**, and schematic illustration of the self-assembly process and Förster resonance energy transfer (FRET) process of **G6⊂4**. Reproduced with permission [35]. Copyright 2023, the Royal Society of Chemistry.

exhibiting stronger fluorescence emission than the monomer in both solution and solid state. They also designed fluorescent guest molecules **G3**, **G4**, and **G5** to interact with **3** (Fig. 2a), forming three host-guest complexes: **G3⊂3**, **G4⊂3**, and **G5⊂3**. These host-guest complexes exhibited highly controllable luminescence. Interestingly, adjusting the host/guest ratio or changing the solvent could produce multiple colors of fluorescence, including white light emission (Fig. 2c, **G4⊂3** with a host/guest molar ratio of 1:4.5).

In 2021, Ma's group [35] constructed a host-guest complex **G6⊂4** using pyrene derivatives **G6** as the guest and *p*-sulfonatocalix[4]arenes **4** as the host. The emission color of the **G6⊂4** changed from indigo blue to cyan due to the excimer formation, and it gradually returned to the indigo blue of the monomer within 72 h (Fig. 3). Additionally, it was also possible to construct a dynamic artificial light-harvesting system by incorporating the cationic energy acceptor ethidium bromide (EB). This system was capable of exhibiting red-blue emission color variations. This time-dependent luminescence provided a direct visual approach into the dynamic processes involved in the self-assembly process.

Similarly, Chen's group [36] reported the water-soluble chiral derivatives of 2,6-helic[6]arene, **5a** and **5b**, which could bind 4-[(4′-*N*,*N*-diphenylamine)-styryl]-*N*-methylpyridinium iodide **G7** to form 1:1 host-guest complex **G7⊂5a** and **G7⊂5b** (Fig. 4). The fluorescence enhancement of host-guest complexes compared to monomeric **G7** could be attributed to the restriction of the ACQ effects. Subsequently, chiral assemblies were obtained based on the

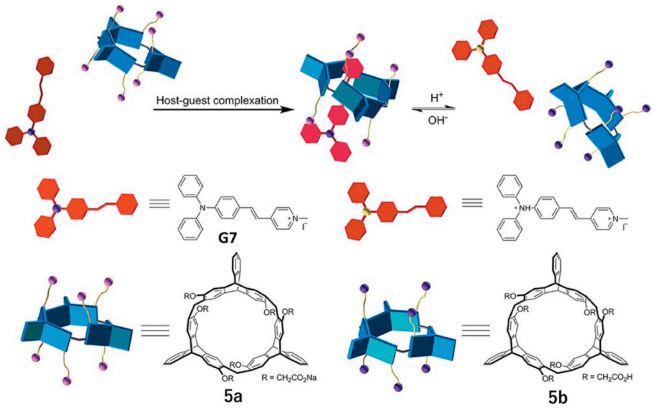

Fig. 4. Chemical structures of **5a**, **5b** and **G7**, and schematic illustration of pH-responsive complex **G7**⊂**5a**. Copied with permission [36]. Copyright 2019, Frontiers Media S.A.

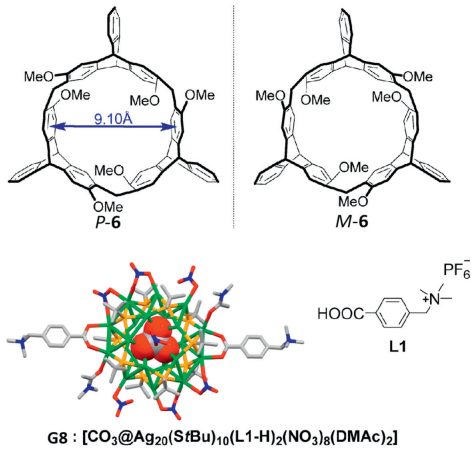

Fig. 5. Chemical structures of *P*/*M*-**6** and **G8.** Copied with permission [37]. Copyright 2022, MDPI.

host-guest interactions, exhibiting clear mirror-image CD and circularly polarized luminescence (CPL) spectra in an aqueous solution. This demonstrated a consecutive chirality transfer from the chiral macrocyclic cavities of **5a** and **5b** to **G7**. Moreover, these assemblies also exhibited responsive CPL activities to the changes in temperature and pH.

In 2022, Chen and coworkers also utilized the enantiomeric 2,6-helix[6]arylene **6** in combination with the nanocluster Ag_{20} (**G8**) through host-guest interactions to create a chiral host-guest complex **G8**⊂**6** (Fig. 5) [37]. This complex exhibited CD property due to the successive chirality transfer from the chiral macrocycles to the achiral silver clusters. Additionally, the singlet excited state of **G8** was encapsulated by the cavity of **6**, resulting in **G8**⊂**6** exhibiting enhanced luminescence properties at room temperature as well as multicolor luminescence with decreasing temperature.

The flexible conformation of macrocyclic arenes results in the racemization of some intrinsic chiral macrocycles due to the rapid transitions between enantiomers. In 2021, Chen's group synthesized saucer[4]arene **7** with strong fluorescent property [38] with quantum yields of 19.6% (Fig. 6a). It was noteworthy that the chiral quaternary ammonium guest **G9** could induce the chirality in the dynamic racemic intrinsically chiral **7**. The resulting host-guest complexes exhibited mirror-image CD signals and CPL property (Fig. 6b), thereby providing a new strategy for the construction of CPL materials through host-guest interactions.

In 2021, Yang and coworkers [39] proposed a strategy to control the photophysical properties of a complex by controlling the

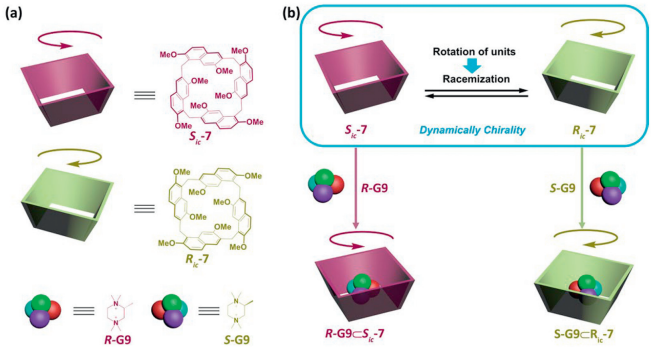

Fig. 6. (a) Chemical structures of S_{ic}/R_{ic}-**7** and *R*/*S*-**G9**. (b) Schematic illustration of competitive conformation chirality of **7** induced by *R*/*S*-**G9**. Reproduced with permission [38]. Copyright 2021, Wiley Publisher.

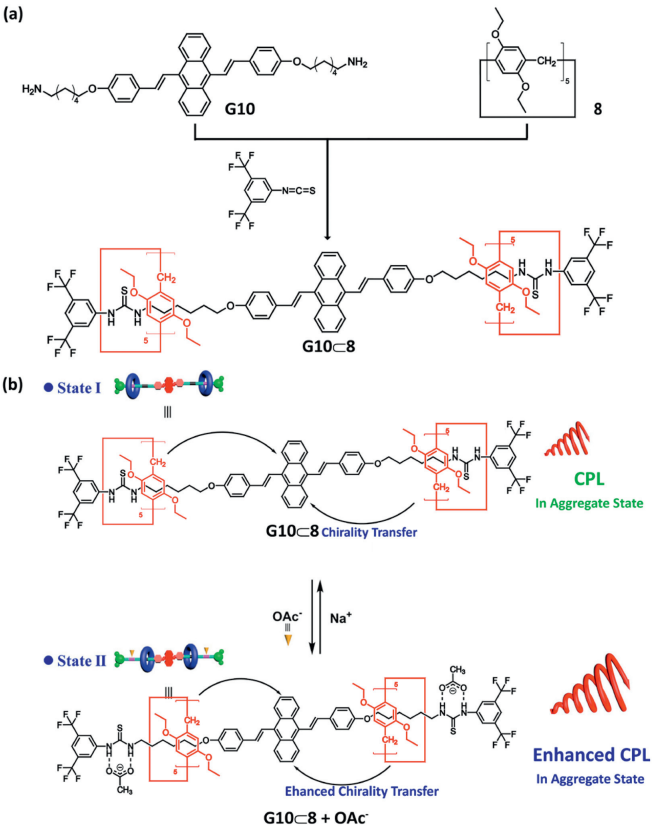

Fig. 7. (a) Synthetic route of **G10**⊂**8**. (b) Schematic illustration of CPL switching system based on **G10**⊂**8** upon the addition or removal of external stimuli. Reproduced with permission [39]. Copyright 2021, Wiley Publisher.

motion of the guest within the cavity of macrocyclic arenes. They designed a CPL switch based on the host-guest complex **G10**⊂**8** (Fig. 7a). By adding and removing acetate anions, they controlled the reversible axial movement of **8** in **G10**⊂**8** along the alkyl chain of guest **G10** to achieve the switch function. This process enhanced the chiral information transfer and regulated the aggregation state of **G10**⊂**8**, resulting in reversible switching between the two CPL emission states with g_{lum} of 2.14×10^{-3} and 1.36×10^{-2} (Fig. 7b).

In 2022, Wei's group [40] used a similar strategy by employing UV-light irradiation to induce the guest phenazine derivatives **G11** to pass through the cavity of the P5, forming the host-guest complex **G11**⊂P5 (Fig. 8a). The fluorescence of **G11**⊂P5 was completely quenched, but the fluorescence emission of **G11** could be

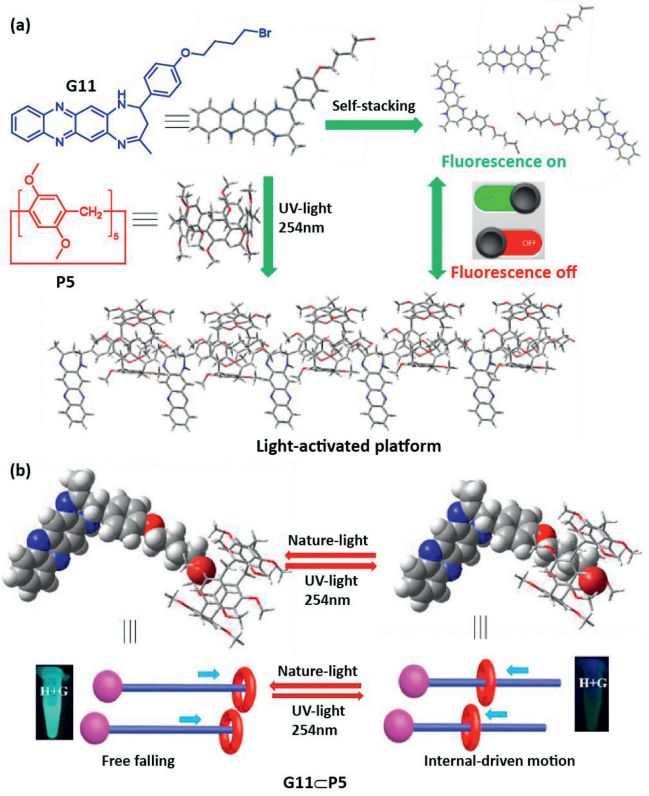

Fig. 8. (a) Chemical structures of P5 and **G11**. (b) Schematic illustration of internal-driven interaction induced by the UV-light (254 nm). Reproduced with permission [40]. Copyright 2022, Elsevier Publishers.

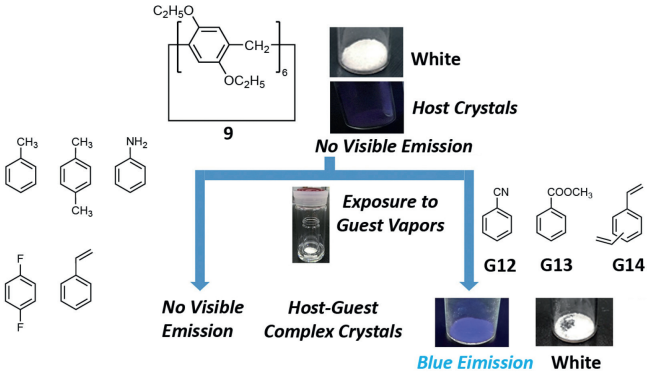

Fig. 9. Vapoluminescence behaviors triggered by crystal-state complexation between **9** and guests (**G12**, **G13**, and **G14**). Reproduced with permission [41]. Copyright 2020, American Chemical Society.

restored upon exposure to natural light due to the free shuttling of **G11** within the cavity of P5 (Fig. 8b).

Due to their electron-rich properties, macrocyclic arenes can act as effective electron donors and form intermolecular charge transfer states when they combined with electron-deficient guests. In 2020, Ogoshi's group [41] reported the vapoluminescence behavior triggered by host-guest complexation in the crystal state. Compound **9** and the guest molecule did not exhibit fluorescence in the visible region when they existed alone. However, in the crystal state, **9** was able to form complexes with guests **G12**, **G13**, and **G14** through host-guest interactions (Fig. 9). These complexes exhibited blue fluorescence, which may be induced by electron transfer facilitated by the host-guest interactions.

In practice, host-guest charge-transfer complexes with strong fluorescence emission are rare because charge transfer usually

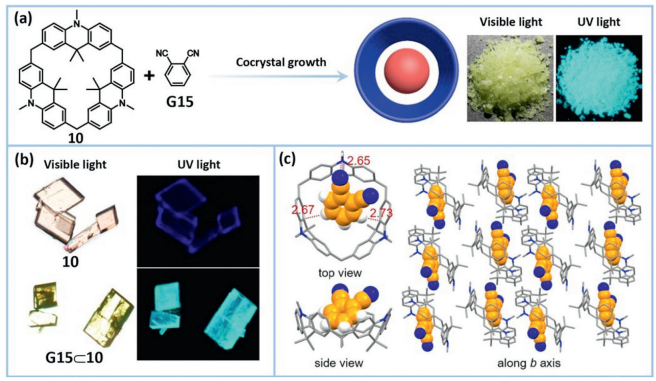

Fig. 10. (a) Preparation of **G15⊂10** by cocrystal growth. (b) Optical microscopy images of **10** and **G15⊂10**. (c) Crystal structures of **G15⊂10**. Reproduced with permission [3]. Copyright 2022, Wiley Publisher.

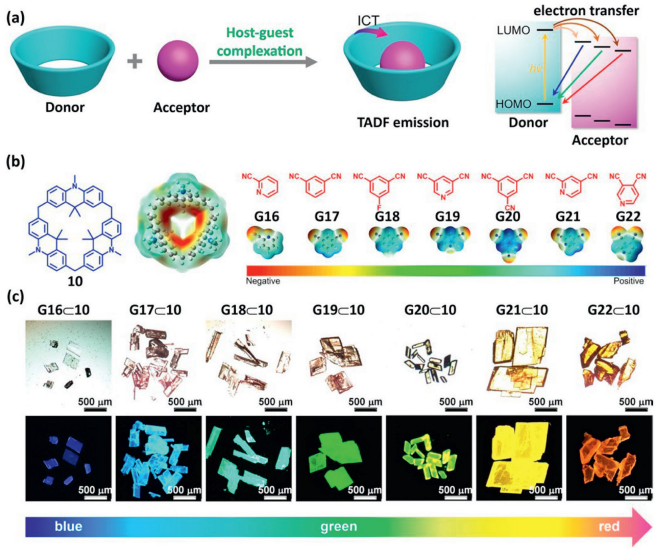

Fig. 11. (a) The TADF emission realized by formation of ICT state between the macrocyclic donor and guest. (b) Chemical structures and electrostatic potential maps of **10** and guests **G16-G22**. (c) Optical microscopy images of **G16⊂10-G22⊂10** under sunlight (up) and UV light (down). Reproduced with permission [42]. Copyright 2024, Springer Nature.

leads to fluorescence quenching upon the formation of the host-guest complex. However, the charge-transfer properties are highly beneficial for thermally activated delayed fluorescence (TADF). In 2022, Chen's group [3] prepared a host-guest cocrystal by utilizing the interaction between calix[3]acridan **10** and **G15** (Fig. 10a). The cocrystal showed green-blue TADF emission due to the strong intermolecular charge transfer (ICT) between **10** and **G15** (Fig. 10b). This was because of the spatial separation of HOMO-LUMO energy level and a small ΔE_{ST} (0.014 eV). Additionally, the photoluminescence quantum yield was as high as 70%.

A general supramolecular strategy for constructing the TADF materials [42] was further proposed. Consequently, they obtained a series of host-guest cocrystals by combining **10** as an electron donor and various guests (**G16-G22**) as electron acceptors (Figs. 11a and b). The cocrystals exhibited efficient TADF properties due to the mediation of multiple non-covalent interactions in the process of intramolecular charge-transfer (ICT). It was noteworthy that the luminescence color of these cocrystals could be continuously tuned from blue to red by finely tuning the electron-withdrawing abilities of the guest molecules (Fig. 11c), achieving a photoluminescence quantum yield of up to 87%. This study provided a general

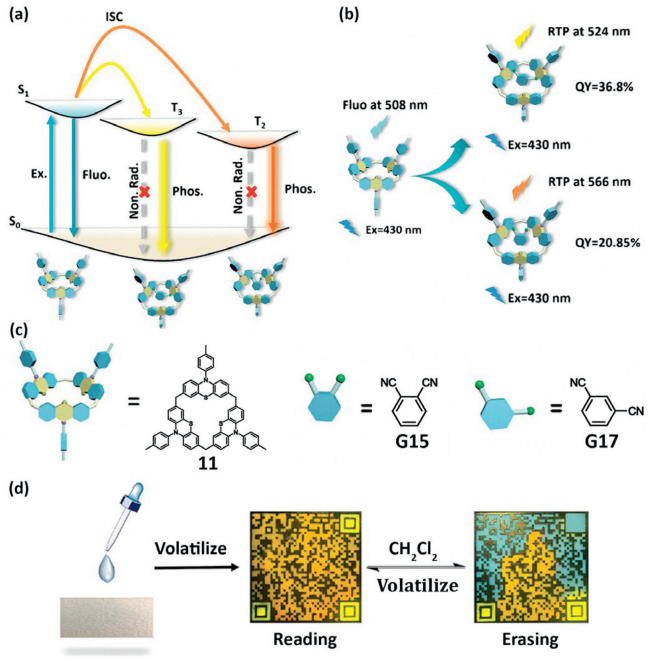

Fig. 12. Schematic illustration of (a) the RTP emission and (b) the RTP emission of selectively activated **11**. (c) Chemical structures of **G15**, **G17**, and **11**. (d) Phosphorescence QR code and information storage/encryption of solvent response. Reproduced with permission [43]. Copyright 2023, Wiley Publisher.

method for the preparation of TADF materials and established a reliable supramolecular strategy for the design of advanced luminescent materials.

Very recently, Liu and his colleagues [43] proposed a novel strategy for preparing two solid-state supramolecular systems with organic room-temperature phosphorescence by using 1,2-/1,3-dicyanobenzene (**G15/G17**) and calix[3]phenothiazine **11** (Fig. 12c). Despite the regular arrangement of **11** in crystals, the vibrational dissipation of the phenyl ring resulted in **11** emitting only 508 nm of fluorescence at room temperature. In contrast, **G15** and **G17** were found to immobilize **11** and inhibit molecular vibrations, thereby reducing the nonradiative relaxation (Fig. 12a). This resulted in the room-temperature phosphorescence (RTP) emission of **11** at 566 nm and 524 nm, respectively (Fig. 12b). Subsequently, they prepared **G15**⊂**11** and **G17**⊂**11** as a Quick Response code (QR code) through solvent evaporation, resulting in a colorful QR code that could be recognized by smartphones under 365 nm UV irradiation. After exposure to dichloromethane vapor, the color of the QR code faded due to the weakening of the interactions between **G15/G17** and **11**, making the code no longer recognizable by cell phones. However, upon solvent evaporation, the colorful QR code reappeared without damage (Fig. 12d). This material exhibits excellent fatigue resistance and allows for multiple conversions.

More recently, Chen's group [44] utilized macrocycle-to-macrocycle conversion to synthesize a novel macrocyclic arene, namely naphth[4]arene **12** (Fig. 13a). This macrocycle could selectively form 1,3- and 1,2-alternate conformations in the solid state. Interestingly, it could assemble with 1,2,4,5-tetracyanobenzene (TCNB) *via* π-π stacking to form two distinct supramolecular crystals: 1,3–**12**@TCNB and 1,2–**12**@TCNB (Fig. 13b). Despite having the same compositions, the conformational change in the macrocyclic arene resulted in different fluorescence property. Co-assembly 1,3–**12**@TCNB exhibited green fluorescence with a quantum yield of 43%, while 1,2–**12**@TCNB exhibited yellow fluorescence with a quantum yield of 45%. Especially, it was further found that depending on the different conformations of **12**, the two co-assemblies

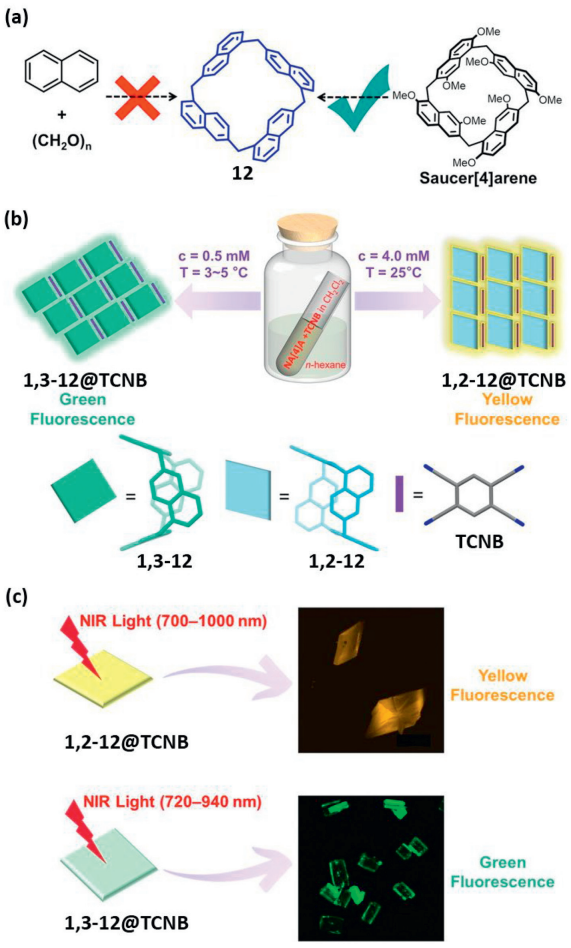

Fig. 13. (a) Macrocycle-to-macrocycle conversion synthetic strategy of **12**. (b) Schematic illustration of the construction of color-tunable supramolecular luminescent co-assemblies 1,3–**12**@TCNB and 1,2–**12**@TCNB. (c) The two co-assemblies excited by NIR light emit distinct upconversion fluorescence. Reproduced with permission [44]. Copyright 2023, Wiley Publisher.

also showed color-tunable two-photon excited up conversion emission due to the intermolecular charge transfer (Fig. 13c).

The modulation of the photophysical properties of fluorescent guests or fluorescent macrocycles by multiple non-covalent interactions within host-guest complexes can facilitate the fabrication of various functional materials. Furthermore, the synthesis of these host-guest complexes is relatively straightforward due to the electron-rich cavities of the macrocyclic arenes and the exo-wall interactions that facilitate the efficient binding of a range of guests. However, these host-guest complexes are poorly processable and typically exist in solution or crystalline, restricting their practical applications.

3. Supramolecular polymers

Supramolecular polymers [45] are polymeric arrays formed by connecting monomeric units through reversible and highly directional non-covalent interactions, such as hydrogen bonding, π-π stacking, and coordination interactions. Benefiting from their facile functionalization and rich host-guest chemistry, macrocyclic arenes are widely utilized in the preparation of supramolecular luminescent polymers. These polymers combine the unique properties of polymers and macrocyclic arenes, and exhibit fascinating reversibility and responsiveness, making them an attractive strategy for the preparation of SLMs.

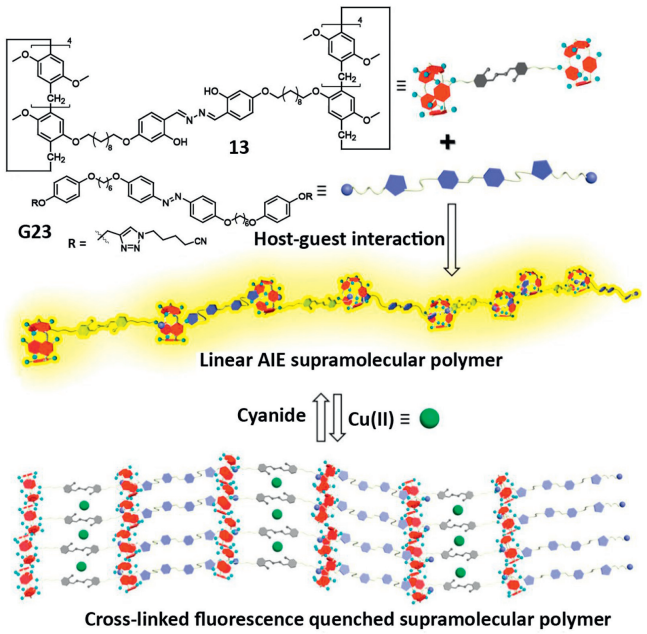

Fig. 14. Chemical structures of **13** and **G23**, and schematic illustrations of the linear AIE supramolecular polymer and the reversible cross-linking process of the linear polymer by Cu^{2+} and CN^{-}. Reproduced with permission [46]. Copyright 2019, American Chemical Society.

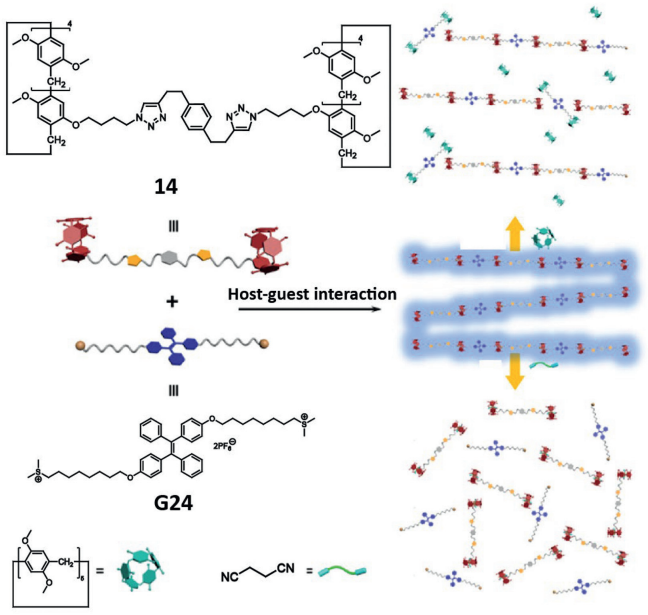

Fig. 15. Chemical structures of **14** and **G24**, and schematic illustration of the formation of linear supramolecular polymer and its dissociation by the addition of 1,4-butanedinitrile and P5. Reproduced with permission [47]. Copyright 2024, Elsevier Publishers.

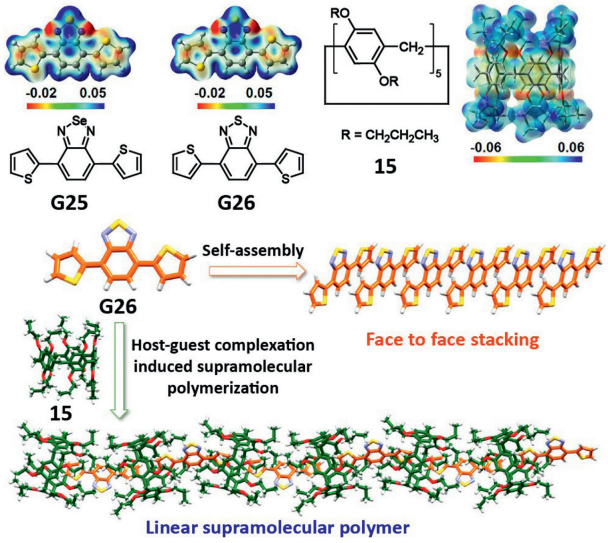

Fig. 16. Chemical structures and distributions of the electrostatic potential mapped onto the electron density surfaces of **G25**, **G26** and **15**, and the self-assembled modes of **G26** and **G26⊂15** in the solid state. Reproduced with permission [48]. Copyright 2020, American Chemical Society.

In 2019, Xia's group [46] introduced a salicylaldehyde azine group into P5, resulting in formation of **13**. Subsequently, they obtained a linear AIE supramolecular polymer through host-guest interaction between **13** and **G23** (Fig. 14). The fluorescence emission intensity of the polymer increased as the increase of the concentrations of **13** and **G23** in chloroform. Additionally, upon drying, the fluorescence was enhanced upon drying due to the closer aggregation of the salicylaldehyde azine groups. Moreover, the salicylaldehyde azine group could coordinate with Cu^{2+}, leading to the cross-linking of the polymer chains and a quenching of the fluorescence. However, the fluorescence could be restored by the addition of cyanide (Fig. 14).

Similarly, Wang's group [47] prepared the linear fluorescent supramolecular polymers with AIE effect based on the host-guest interaction between P5 derivative **14** and TPE derivative **G24**. These polymers showed significantly enhanced fluorescence emission compared to that of free **G24**. Simultaneously, introducing competitive molecules such as 1,4-butanedinitrile and P5 into the system triggered the disruption of the polymer, leading to fluorescence quenching (Fig. 15). Furthermore, this supramolecular polymer could detect Pb^{2+} due to the presence of a triazole group in **14**, which coordinated with Pb^{2+} and led to a reduction in the fluorescence intensity of the polymer.

In 2020, Huang's group [48] introduced another method to enhance the fluorescence emission in supramolecular polymers. They used supramolecular polymerization to regulate the aggregation and emission behaviour of dyes in the solid-state. By utilizing the host-guest interaction between guests **G25** or **G26** and the pillar[5]arene derivative **15**, they prepared linear fluorescent supramolecular polymers. The polymerization process reorganized the parallel arrangement of **G25** or **G26** into a well-organized head-to-tail structure (Fig. 16). This reorganization suppressed the ACQ effect and significantly improved the photoluminescence efficiency of the polymer. Additionally, the system exhibited two-photon emission property.

Moreover, supramolecular polymers can be prepared from self-complementary monomers, which are constructed by covalently attaching the guest fragment to the macrocyclic arenes. In 2021, Qu and co-workers [49] connected the oxazolo[4,5-*b*]phenazine-2-thiol group to P5 through covalent bonds and obtained monomer **16** (Fig. 17). A linear supramolecular polymer with fluorescent property was then formed through host-guest interactions between the cavity of P5 and the oxazolo[4,5-*b*]phenazine-2-thiol group in $CHCl_3$. Due to the excellent processability of this fluorescent supramolecular polymer, fluorescent thin films were further prepared. These films exhibited vapochromic behaviour and were effectively used for the direct detection of aliphatic aldehyde micropollutants.

Recently, Qu's group [50] modified the TPE and nitrile groups at both rims of P5 to obtain monomer **17**. Subsequently, supramolec-

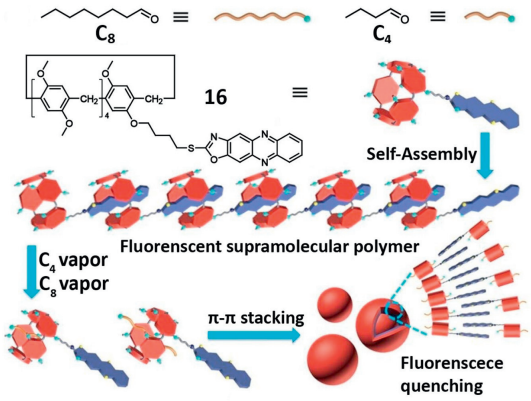

Fig. 17. Chemical structure of **16** and schematic illustration of the formation of the fluorescent supramolecular polymer and its application in the detection of *n*-butyraldehyde (C_4) and caprylicaldehyde (C_8) vapors. Reproduced with permission [49]. Copyright 2022, Wiley Publisher.

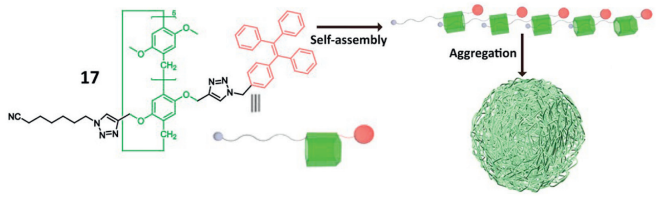

Fig. 18. Chemical structure of **17** and schematic illustration of the construction of the luminescent spherical aggregates based on the self-assembly of **17**. Reproduced with permission [50]. Copyright 2023, the Royal Society of Chemistry.

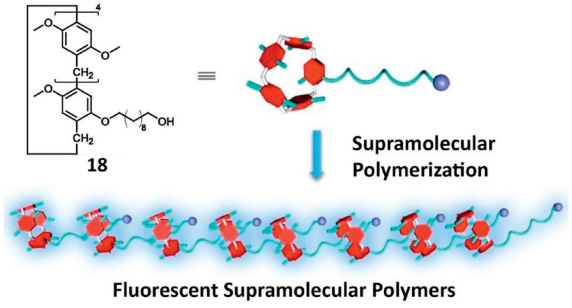

Fig. 19. Chemical structure of **18** and schematic illustration of linear supramolecular polymers. Reproduced with permission [51]. Copyright 2023, Wiley Publisher.

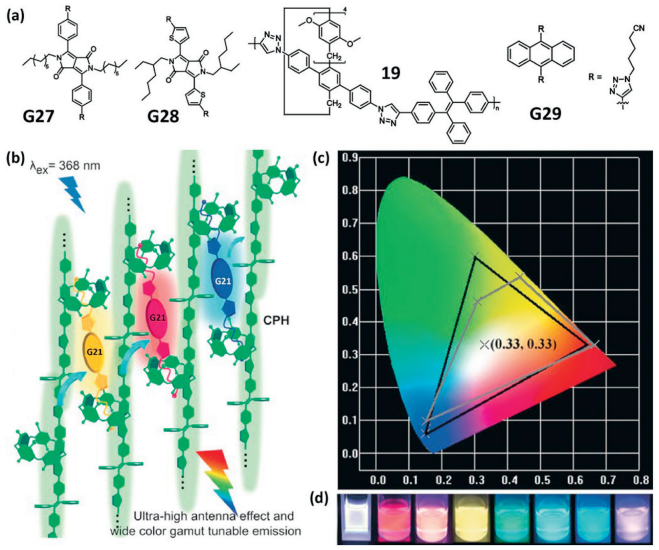

Fig. 20. (a) Chemical structures of **19**, **G27**, **G28** and **G29**. (b) Schematic illustration of supramolecular polymer network. (c) CIE 1931 chromaticity diagram. Gray quadrilateral: the color gamut of the supramolecular polymer network. Black triangle: the sRGB gamut. (d) Fluorescence photographs of the supramolecular polymer network in the co-solvent of $CHCl_3$/cyclohexane (3:7 by volume), including a white emission of (0.33, 0.33) in CIE coordinates. $\lambda_{ex} = 368$ nm. Reproduced with permission [52]. Copyright 2020, Wiley Publisher.

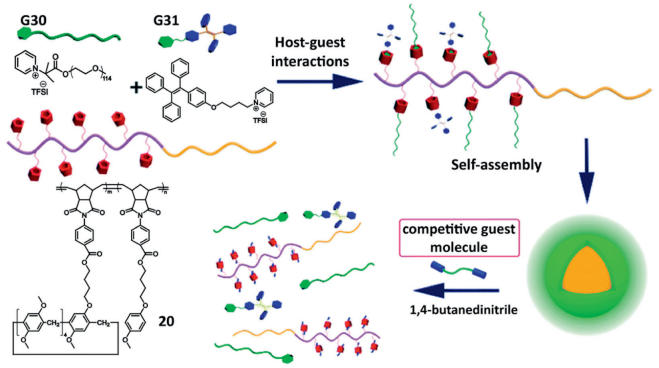

Fig. 21. Chemical structures of **20**, **G30** and **G31**, and schematic illustration of the supramolecular material constructed by host-guest interactions. Reproduced with permission [53]. Copyright 2022, the Royal Society of Chemistry.

ular polymers were prepared based on the host-guest interactions between the nitrile group and P5 (Fig. 18). These supramolecular polymers exhibited significant AIE effect due to the restricted intramolecular rotation of the TPE groups. Moreover, the polymer was able to further self-assemble in THF/H_2O mixed solvent to form spherical aggregates.

In 2023, Li's group [51] constructed a supramolecular polymer that did not require conventional chromophores. They obtained linear supramolecular polymers by the self-assembly of **18** in solution. The rigid structure of the P5 contributed to the increased rigidity of the supramolecular polymer (Fig. 19), which impeded the movement of the polymer chains, reduced the non-radiative relaxation and endowed the polymer with photoluminescent properties.

Another approach for preparing supramolecular polymers based on host-guest interactions of macrocyclic arenes is to introduce macrocyclic arenes into the covalent polymers and then form supramolecular crosslinked networks by host-guest interactions. In 2020, Tang's group [52] synthesized a covalent polymer **19** with P5 and TPE units incorporated into the molecular backbone. Due to the host-guest interactions, various conjugated ditopic guests (**G27**, **G28**, and **G29**) could be sequestered between the polymeric host chains without experiencing ACQ (Fig. 20a). Additionally, the polymer chains could be entangled with each other or form supramolecular crosslinks network through binding with the guest molecules to achieve aggregation-induced emission (Fig. 20b). In addition, using **19** as the donor and **G27**, **G28** and **G29** as the acceptors, the supramolecular polymer network exhibited remarkably efficient energy transfer. It exhibited a high antenna effect of 35.9 in solution and 90.4 in solid film. Furthermore, by modifying the molecular structures of the acceptors and donors or adjusting their ratio, the emission characteristics of the supramolecular polymer network could be tuned (Fig. 20d). This resulted in a color gamut covering approximately 96% of the sRGB area, including an accurate white emission at (0.33, 0.33) in CIE coordinates (Fig. 20c).

Subsequently, Liao's group [53] obtained covalent polymer **20** with P5 side chains and employed a similar strategy to introduce pyridinium salts containing polyethylene glycol (**G30**) and TPE (**G31**) into **20** *via* host-guest interaction (Fig. 21). The polymers were then able to self-assemble in solution to form micelles and

exhibited an AIE effect with increased fluorescence intensity. Moreover, the addition of the competitive guest 1,4-butanedinitrile resulted in a decrease in fluorescence intensity, which was attributed to the disruption of the micelle structure.

More recently, Chen's group [54] constructed a color-tunable TADF polymer *via* ICT interaction between the calix[3]acridan-modified polymer with various acceptors (Fig. 22a). The TADF properties of the polymers were due to through-space charge transfer between the macrocyclic donor and the electron-deficient guests (**G17**, **G18**, **G20**, **G21**). In particular, by modifying the electron-withdrawing capacity of the guests, they were able to achieve multi-color emission and achieve a PLQY of up to 40%. Furthermore, the polymers displayed favourable processability, stability and tunability. Based on these properties, they created anti-counterfeiting labels on various substrates and constructed multi-color two-dimensional barcodes that could be scanned and read by smart devices (Fig. 22).

Macrocyclic arenes can also form supramolecular polymers with metal ions through coordination due to the ease of functionalization. Yang's group [55] synthesized a color-tunable supramolecular polymer using **21** as the ligand and Eu^{3+} and Tb^{3+} as metal ions. Due to its inherent blue fluorescence and electron-rich structure, **21** played a dominant role in the blue emission of the polymer and served as an excellent energy donor for lanthanide metal ions. The concentrations of Eu^{3+} and Tb^{3+} could determine the red and green intensity of the system, respectively. Consequently, by adjusting the molar ratio of Eu^{3+} and Tb^{3+}, the fluorescence color of the polymer can be tuned from red to green. Moreover, the polymer exhibited white light emission at a molar ratio of 1:3 (Fig. 23) and could selectively detect nitroaromatic pollutants through the electron transfer mechanism.

In a recent study, Tang and colleagues [56] integrated the planar chirality of P5 with the AIE effect of TPE through coordination interactions. They synthesized macrocycle **22**, where the TPE units provided the AIE effect, and the spatial effects restricted the rotation of the benzene units in the P5. They then obtained a pair of optically pure enantiomers, *pR*-**22** and *pS*-**22**. Supramolecular polymers were created by coordinating *pR*-**22**/*pS*-**22** with silver ions (Fig. 24a). This coordination led to a 1.5-fold enhancement in the CD signal and an increase in the quantum yield from approximately 0.9 to 2.0. The enhancement of chiral and fluorescent properties allowed the *pR*-polymers and *pS*-polymers to exhibit significant CPL property in dilute solution, with g_{lum} values of 1.30×10^{-4} and -0.65×10^{-4}, respectively. Notably, the polymers formed aggregates in aqueous media (Fig. 24b), resulting in a more than a 25-fold increase in quantum yield compared to their solution state. Additionally, the g_{lum} value of the *pR*-aggregates increased to 2.69×10^{-3}, representing a 21-fold enhancement compared to that of the *pR*-polymers.

In 2020, Shi's group [57] synthesized a P5 derivative **23** containing two pyrene groups. This compound formed a linear supramolecular polymer by π-π stacking due to the large conjugated structure of pyrene. The fluorescence of the polymer changed from blue to green as the concentration of **23** or solvent polarity increased. Later, the researchers introduced the red emissive Eu-terpyridine complex **G32** into the system. Through the host-guest interaction between the P5 and **G32**, a supramolecular network was formed. By adjusting the concentration and solvent polarity, this network exhibited white light emission and tunable fluorescence (Fig. 25).

In 2023, Liu and co-workers [58] reported a full-color supramolecular switch. The system was assembled through various non-covalent interactions involving 2,6-pyridine dicarboxylic acid-modified P5 (**24**), lanthanide ions (Tb^{3+} and Eu^{3+}), and a dicationic diarylethene derivative (**G33**). By adjusting the molar ratio of Tb^{3+} and Eu^{3+} within the system, they achieved full-color luminescence,

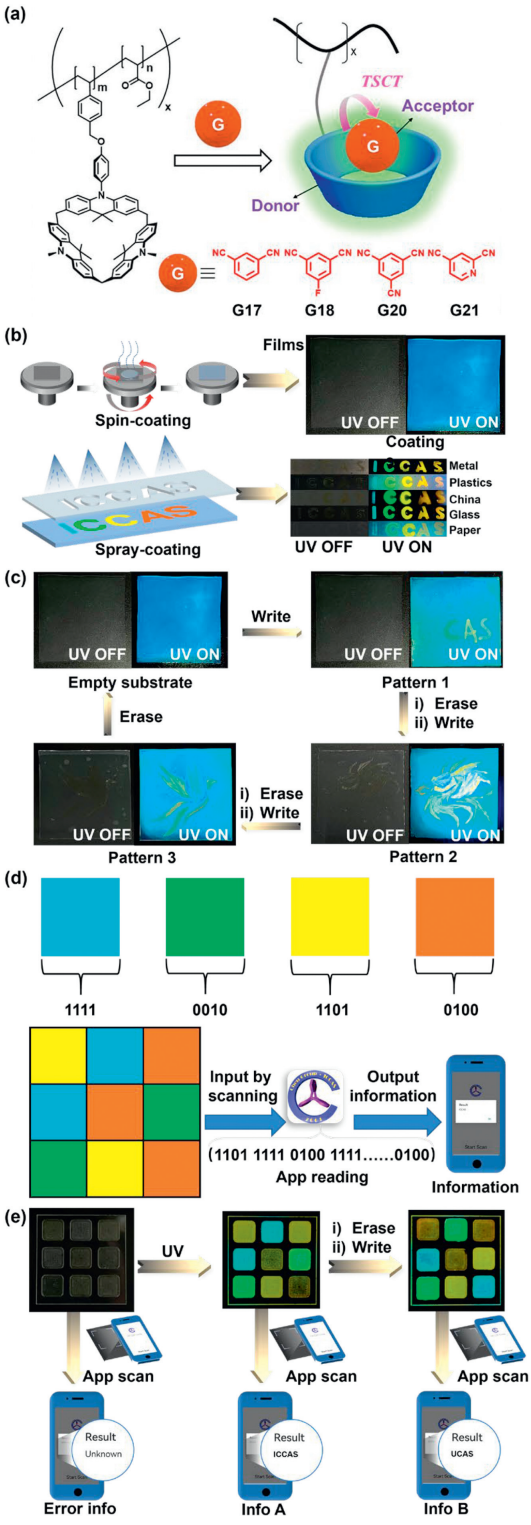

Fig. 22. (a) Chemical structures of the color-tunable TADF polymers. (b) Schematic illustration of thin films prepared by spin-coating method and coatings prepared by spray-coating method. (c) The process of multiple reuses of anti-counterfeit labels (pattern 1: ♥CAS; pattern 2: dragon; pattern 3: phoenix) produced by TADF polymers. (d) Schematic illustration of binary information conversion of multi-color two-dimensional barcode. (e) A conceptual application of multi-color two-dimensional barcode.

including white light emission in dichloromethane (CIE: 0.31, 0.33) and aqueous (CIE: 0.31, 0.32) solutions. Furthermore, the interconversion between **G33a** and **G33b** was controlled by alternating UV/visible light irradiation, demonstrating the capability to control the fluorescence switch of the polymer (Fig. 26). This supramolec-

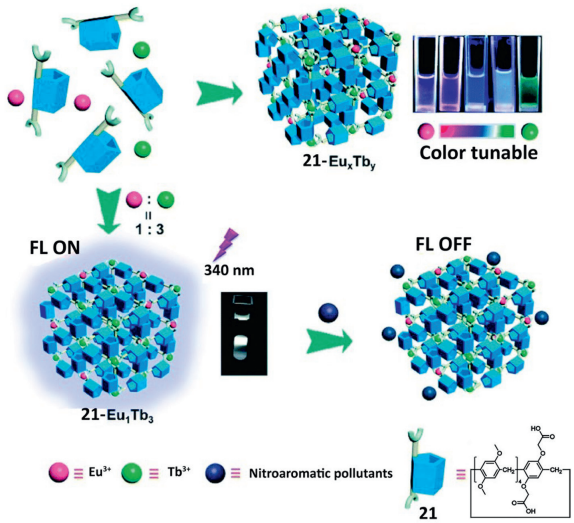

Fig. 23. Chemical structure of **21** and schematic illustrations of the color-tunable polymer constructed by tuning the molar ratio of Eu^{3+} and Tb^{3+} in the system and the fluorescence on/off sensing of nitroaromatic pollutants. Reproduced with permission [55]. Copyright 2022, the Royal Society of Chemistry.

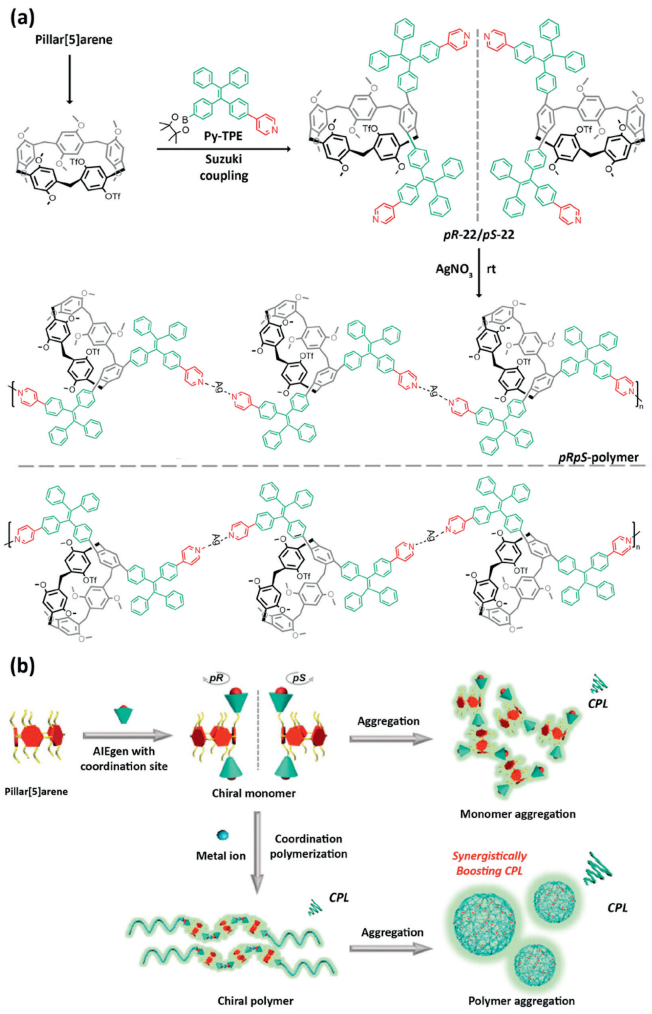

Fig. 24. (a) Chemical structures and synthetic routes of *pR*/*pS*-**22** and the corresponding coordination supramolecular polymers. (b) Schematic illustration of the construction of P5-based materials with polymerization and aggregation enhanced CPL. Reproduced with permission [56]. Copyright 2023, Wiley Publisher.

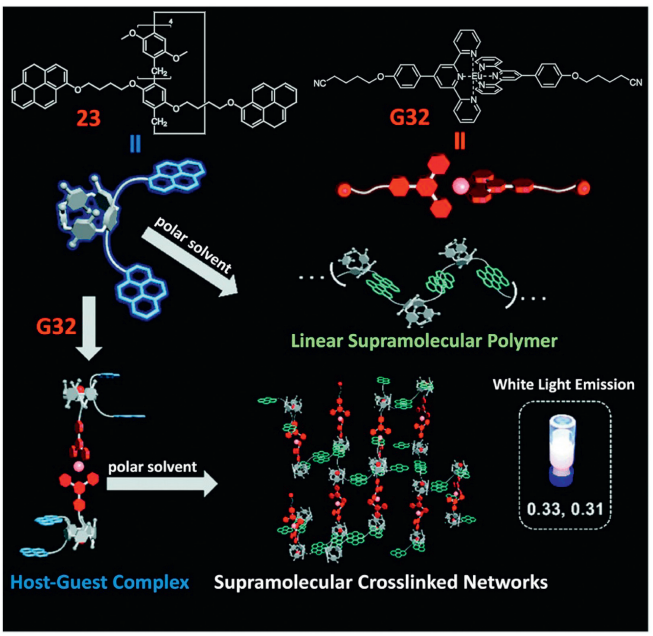

Fig. 25. Chemical structures of **23** and **G32**, and schematic illustration of solvent-controlled aggregation of **23** and the modulation process of white emission. The inset picture shows the white fluorescence of the supramolecular system under UV light. Reproduced with permission [57]. Copyright 2020, the Royal Society of Chemistry.

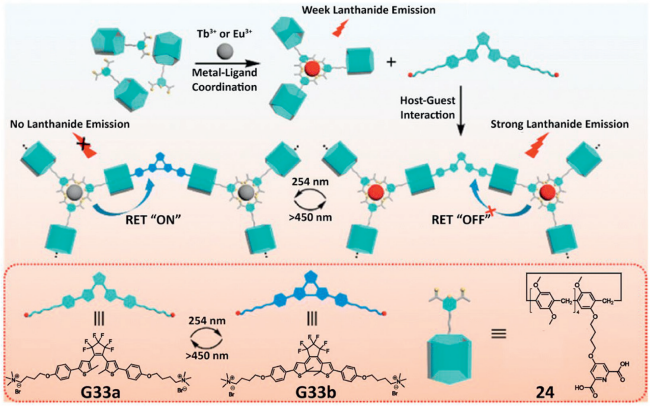

Fig. 26. Chemical structures of **24**, **G33a** and **G33b**, and schematic illustration of the construction of a full-color lanthanide supramolecular light switch based on noncovalent assembly. Reproduced with permission [58]. Copyright 2023, the Royal Society of Chemistry.

ular polymer was successfully applied to anti-counterfeiting by using intelligent multi-colored writing inks.

Recently, Wang's group [59] combined **25** and **G34** *via* host-guest interactions to obtain [3]pseudorotaxane (Fig. 27a). This was followed by the formation of a supramolecular fluorescent polymer crosslinked network through hydrogen bonding between Schiff-base groups and van der Waals forces between cholesterol groups (Fig. 27b). Moreover, the reversible metal coordination between the Schiff-base groups induced by cyanide ions and Cu^{2+} enabled the system to exhibit fluorescence switching (Fig. 27b). Utilizing the surface binding capability of the supramolecular polymer and the fluorescence emission properties of Schiff-base groups, they prepared rewritable fluorescent paper by dip-coating polymer on cellulose paper. This paper allowed for cyclic writing with Cu^{2+} ions as ink and CN^- ions as erasers (Fig. 27c).

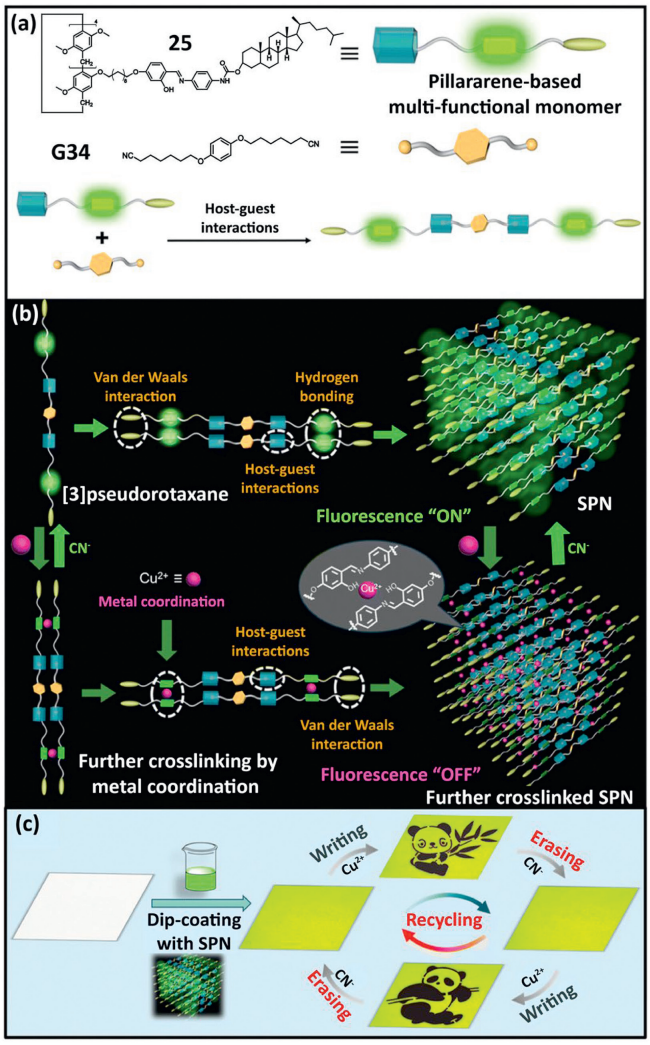

Fig. 27. (a) Chemical structures of **25** and **G34**. Schematic illustration of (b) two supramolecular polymer networks (SPNs) and the reversible quenching and recovery property of the fluorescence by Cu^{2+} and CN^- ions, and (c) the recyclable writing and erasing processes of SPN-based rewritable paper. Reproduced with permission [59]. Copyright 2023, the Royal Society of Chemistry.

Stimulus responsiveness is one of the most important features of supramolecular luminescent polymers due to the dynamic and reversible non-covalent interactions. In recent years, Yang and his colleagues [60–63] have reported a variety of stimuli-responsive fluorescent supramolecular polymers.

In 2019, they designed a [2]biphenyl-extended pillar[6]arene **26** [60], which was used as a building block in the synthesis of a supramolecular polymer through the host-guest interaction between **26** and the TPE derivative **G35**. In the presence of Hg^{2+}, the polymer formed a supramolecular network and self-assembled into spherical nanoparticles due to the coordination between Hg^{2+} and thymine on the edge of **26**. This process restricted the intramolecular rotation of **G35**, leading to supramolecular assembly-induced emission enhancement, and exhibited strong AIE fluorescence (Fig. 28). The polymer had the potential for the fluorescence detection of Hg^{2+} and the efficient removal of Hg^{2+}, with a rapid adsorption rate and high adsorption capacity. Remarkably, the polymer could be effectively regenerated and recycled without any loss by simple treatment with Na_2S.

Recently, they [63] synthesized a supramolecular polymer network with AIE emission using **27** and a homoditopic guest **G36** (Fig. 29). In addition, they prepared a Fe^{3+} ion responsive film

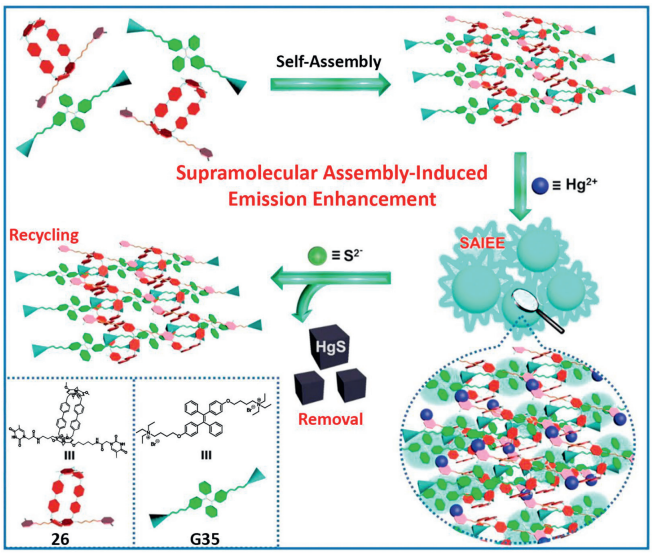

Fig. 28. Chemical structures of **26** and **G35** and schematic illustration of the sensing and removal of Hg^{2+} from water based on the "switch-on" fluorescence of the supramolecular polymers and the regeneration–recycling process. Reproduced with permission [60]. Copyright 2019, American Chemical Society.

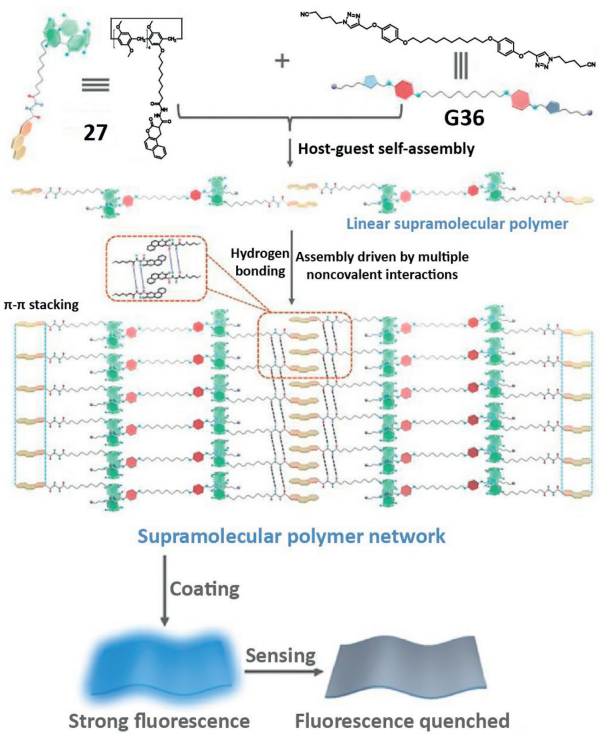

Fig. 29. Chemical structures of **27** and **G36**, and schematic illustrations of the assembly process of supramolecular polymer and the sensing to Fe^{3+}. Reproduced with permission [63]. Copyright 2023, Elsevier Publishers.

based on the polymer. Upon the addition of Fe^{3+} to the system, **27** and Fe^{3+} formed a non-emissive 1:1 complex due to coordination (Fig. 29), enabling the selective detection of Fe^{3+} with lowest detection limit (LOD) of 3.0×10^{-6} mol/L.

Supramolecular polymers based on macrocyclic arenes can also form supramolecular gels [25,64]. In 2022, Chen's group [65] introduced CPL property into the supramolecular polymers. They synthesized a pair of enantiomeric bishelic[6]arenes **28** (Fig. 30a). Through host-guest interactions, **28** could form linear supramolecular polymers with two achiral luminescent guests, **G37** and **G38**,

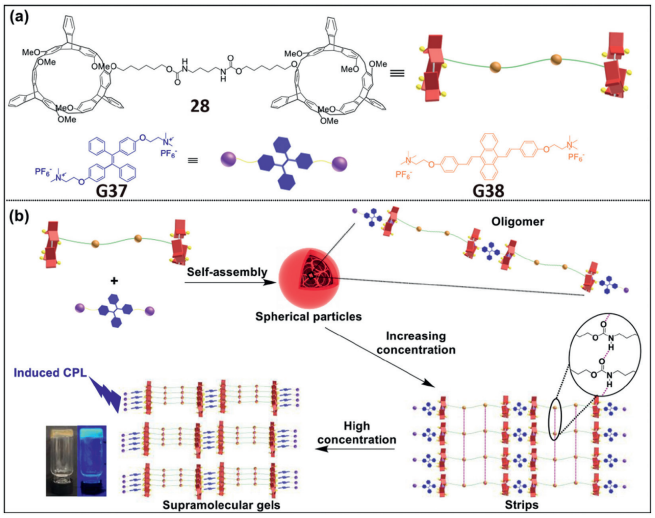

Fig. 30. (a) Chemical structures of **28**, **G37**, and **G38**. (b) Schematic illustration of the supramolecular polymerization based on host-guest interaction and hydrogen bonding (inset: photo of the supramolecular gels under natural light and 365 nm UV light). Reproduced with permission [65]. Copyright 2022, American Chemical Society.

which exhibited enhanced fluorescence and induced CD property. As the concentration of the polymer increased, the linear supramolecular polymer could transform into a gel through the synergistic effect of hydrogen bonding and host-guest interactions, accompanied by a significant enhancement of the induced CD property. Furthermore, the supramolecular gels exhibited CPL property as a result of the efficient chiral transfer from **28** to **G37** and **G38** (Fig. 30b). Remarkably, by adjusting the ratio of the two guests, chiral supramolecular gels with white light emission with a g_{lum} value of about 1.3×10^{-3} were obtained.

In the preceding years, Wei and coworkers have prepared a variety of stimuli-responsive supramolecular polymer gels and utilized them for the detection and separation of a diverse range of metal ions and pollutants [66–72]. In 2019, they successfully constructed a gel [69] with AIE property by introducing multiple interaction sites and assembling a bisnaphthalimide-functionalized P5 **29** and a 4,4′-bipyridinium salt **G39** (Fig. 31). The gel demonstrated the capacity to sense a broad spectrum of pollutants, including organic dyes, organic pollutants, volatile organic compounds, and so on. Additionally, it exhibited the ability to separate these pollutants, with a separation rate of heavy metal ions, metal oxides, various organic dyes, and organic pollutants reaching 99.8%.

Recently, they synthesized phenazine-bridged P5 **30** and naphthalene diimide **G40** [72], which could self-assemble into spherical structures in dilute solution through host-guest interactions, exhibiting yellow fluorescence. Furthermore, the spherical structure transformed into a supramolecular polymer gel with the increase of concentration (Fig. 32). Subsequently, a novel biogenic amine-responsive platform was obtained based on this gel by adjusting the concentration of the host and guest. This platform is sensitive to most amine compounds and can detect alkaline amine gas or liquid amine in solid, solution, and gel states.

Supramolecular polymers based on macrocyclic arenes have excellent processability, recyclability, and self-healing properties. Furthermore, the host-guest interactions between the macrocyclic arenes and guests facilitate the entry of these supramolecular polymeric materials into the field of environmentally responsive materials. However, the synthesis process of these polymers is relatively complex, and the starting materials are not commercially available. Consequently, it is challenging for macrocyclic arenes-based supramolecular polymers to realize their full potential in practical applications, at least for the time being.

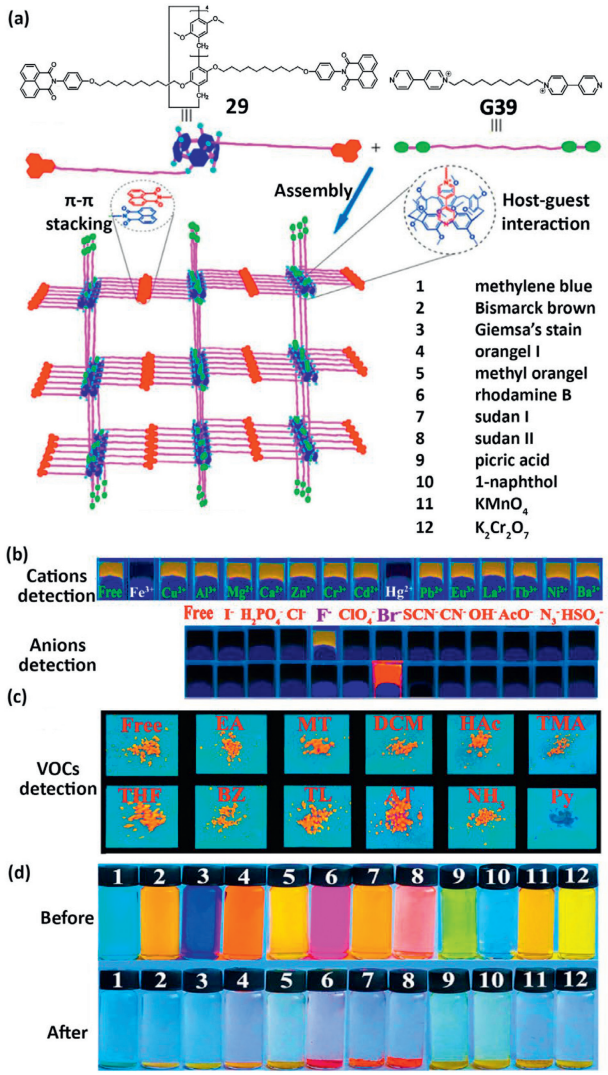

Fig. 31. (a) Chemical structures of **29** and **G39**, and possible assembly mechanism of the gel and photo showing the broad-spectrum detection and adsorption separation properties for broad-spectrum pollutants for (b) cations and anions, (c) volatile organic compounds (VOCs), and (d) various organic dyes, organic pollutants, and oxyanions. Reproduced with permission [69]. Copyright 2019, American Chemical Society.

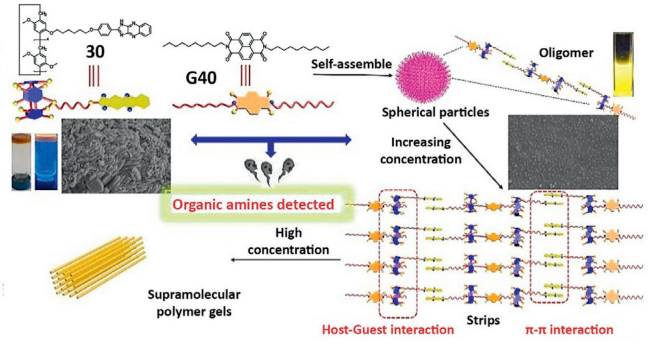

Fig. 32. Chemical structures of **30** and **G40**, and schematic illustration of the assembly process between **30** and **G40** and its response mechanism. Reproduced with permission [72]. Copyright 2023, Elsevier Publishers.

4. Supramolecular nanoparticles

In recent years, supramolecular nanoparticles (SNs) have been widely used in drug delivery [73], bioimaging and cancer therapy

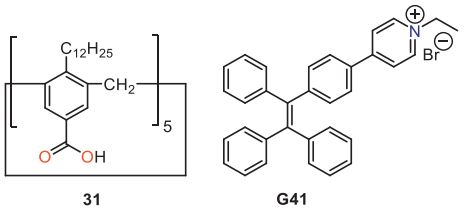

Fig. 33. Chemical structures of **31** and **G41**.

[74]. Macrocyclic arenes have become essential in the preparation of these SNs [30,75] due to their inherent cavities and facile functionalization.

In 2020, Ding's group [75] reported a method to prepare supramolecular AIE nanodots using the host-guest interaction between calix[5]arene **31** (Fig. 33) and aggregation-induced emission luminogens (AIEgens). The co-assembly between the two components constrained the intramolecular motions of AIEgens, reducing ISC and thermal inactivation pathways. The AIE dots, loaded with **G41** (Fig. 33), exhibited an exceptionally high quantum yield of 0.72. Additionally, the researchers found that the AIE nanodots had minimal side effects *in vivo*, indicating their potential as ultrasensitive fluorescent imaging agents for guiding cancer surgeries through *in vivo* studies of peritoneal carcinomatosis mouse models.

Shen's group [76] developed a host-guest complex using carboxylate-modified P5 **32** as the host and **G42**, which had a tetraphenylethene core, as the guest. The fluorescence intensity of this complex was significantly higher compared to free **G42**. They used a nanoprecipitation method to create SNs with enhanced fluorescence emission (Fig. 34a). Intriguingly, these SNs could encapsulate doxorubicin (DOX), and the fluorescence of the system was quenched due to FRET and ACQ effects. When DOX was released intracellularly, the fluorescence of the SNs was restored, allowing for *in situ* visualization of drug release (Fig. 34b). Furthermore, the nanoparticles retained the anticancer efficacy of DOX, indicating their potential for application in cancer therapy.

In the same year, Hu's group [77] introduced tetrastyrene into the backbone of the pillar[5]arenes to obtain a water-soluble pillar[5]arenes **33** (Fig. 35), which combined both the AIE effect and the host-guest property. It could bind with DNS-G (obtained by using SN-38) to form AIE-SNs based on host-guest interactions and fluorescence resonance energy transfer. The nanoparticles were employed to construct a glutathione (GSH)-responsive supramolecular drug delivery system with yellow fluorescence emission. The system was capable of releasing SN-38 efficiently at high GSH concentrations in the microenvironment of tumor cells, which was anticipated to be utilized for cancer therapy.

Realizing reversible control of morphological transformation between various nano-assemblies is very important in the field of smart materials. In 2020, Yao and co-workers [78] constructed SNs based on the host-guest interactions of **34** and a bicyanostilbene derivative **G43**. These SNPs exhibited a two-step sequential fluorescence enhancement (Fig. 36). Initially, **G43** formed nanofibers in an aqueous solution with weak fluorescence, which transformed into nanosheets with enhanced fluorescence upon the addition of **34**. Subsequently, the interaction with sodium dodecylbenzene sulfonate (SDBS) further enhanced the fluorescence, forming nanoparticles that could specifically target mitochondria in live cells with the help of the target molecule HDPP, making them useful for cellular imaging applications.

In 2021, Wei and his colleagues [79] reported a method to control the reversible transformation between nanoparticles and nanofilm. They designed and synthesized a tri-[2]rotaxane based on **35** and **G44**. Tri-[2]rotaxane could self-assemble into nanoparticles, which could be reversibly transformed into nano-film by the addition of trimethylamine and suberic acid alternately (Fig. 37). Moreover, the fluorescence of the tri-[2]rotaxane showed an "off-on-off" switching behavior.

Transformation of the morphology of the nano-assemblies can also be used for detection. Zhang's group [80] recently used water-soluble pillar[5]arene **34** and guest **G45** to construct fluorescent nanoparticles, which exhibited strong fluorescence emission in aqueous solution. When L-glutamic acid (L-Glu) and L-aspartic acid (L-Asp) were present in solution, the SNPs were converted into

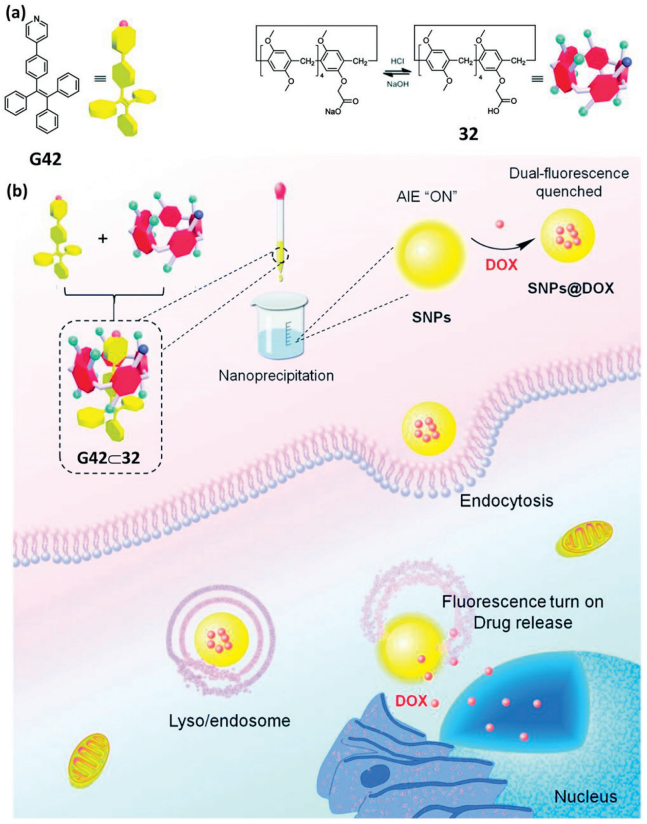

Fig. 34. (a) Chemical structures of **32** and **G42**. (b) The fabrication of SNPs@DOX using SNPs as drug nanocarriers and schematic illustration of imaging-guided drug delivery. Reproduced with permission [76]. Copyright 2021, the Royal Society of Chemistry.

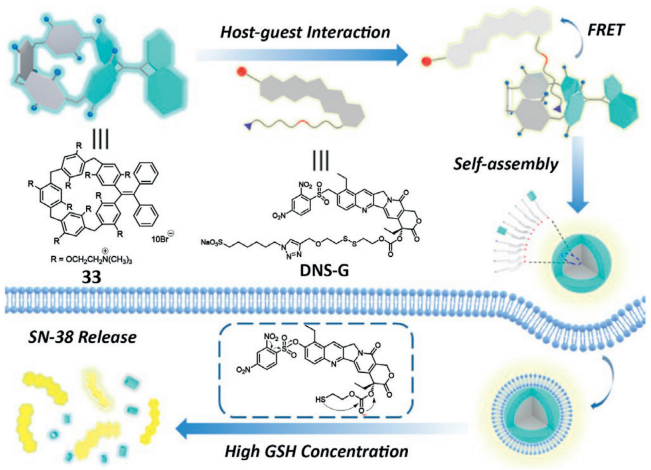

Fig. 35. Chemical structures of **33** and DNS-G, and schematic illustrations of the formation of SNs and their stimuli-responsive drug release. Reproduced with permission [77]. Copyright 2021, American Chemical Society.

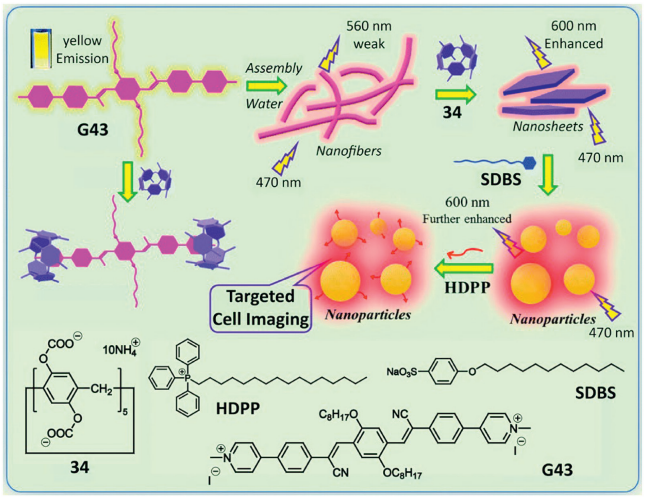

Fig. 36. Chemical structures of **34**, **G43**, SDBS and target molecule (HDPP), and schematic illustration of supramolecular self-assemblies from **G43**, **34**/**G43**, and **34**/**G43**/SDBS. Reproduced with permission [78]. Copyright 2020, the Royal Society of Chemistry.

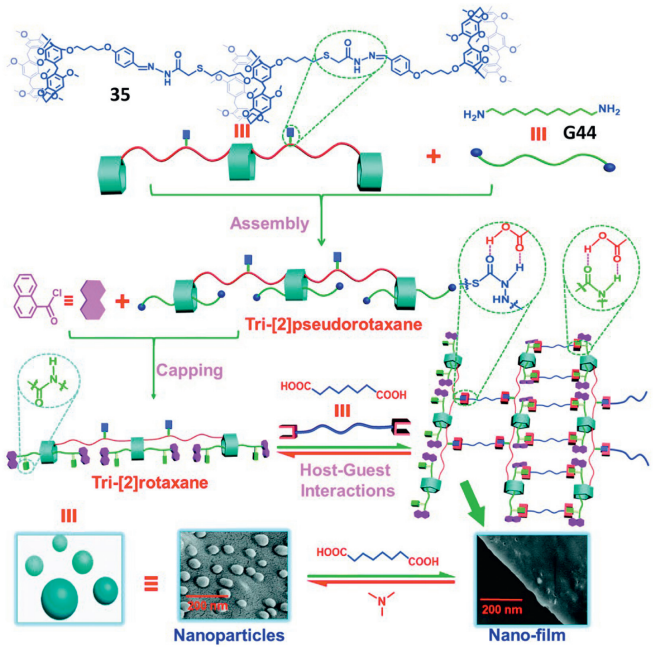

Fig. 37. Chemical structures of **35** and **G44**, and schematic illustration of constructing nano-film by the guest induction to regulate fluorescent nanoparticles that formatted from the tri-[2]rotaxane. Reproduced with permission [79]. Copyright 2021, the Royal Society of Chemistry.

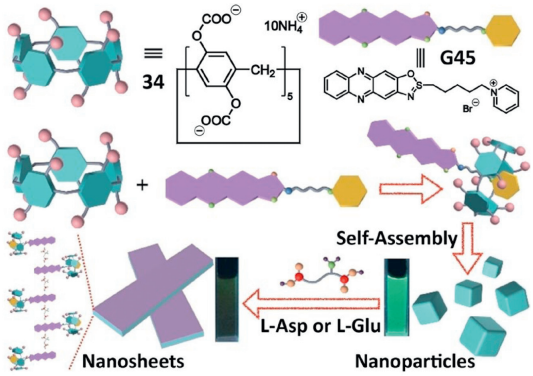

Fig. 38. Chemical structure of **G45** and schematic illustrations of the construction of fluorescent nanoparticles and its application in detection of L-Asp and L-Glu in water. Reproduced with permission [80]. Copyright 2022, Wiley Publisher.

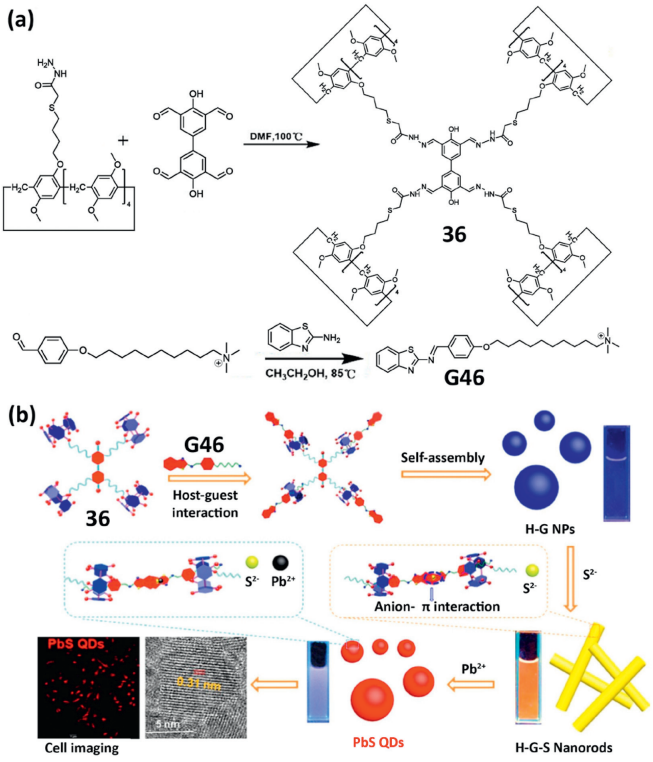

Fig. 39. (a) Synthetic routes of **36** and **G46**. (b) Schematic illustration of the proposed assembly mode of the supramolecular system and ions inducing them to transition from the nanomaterials to QDs. Reproduced with permission [81]. Copyright 2022, American Chemical Society.

weakly fluorescent nanosheets (Fig. 38), resulting in highly selective detection of L-Glu and L-Asp with LODs of 4.03×10^{-7} mol/L and 2.09×10^{-7} mol/L, respectively.

A strategy for *in situ* detection of $Pb^{2+}$was recently reported by Lin's group [81]. They first synthesized the P5 derivative **36** (Fig. 39a), which in aqueous solution was able to self-assemble with the guest **G46** in aqueous solution to form nanoparticles without fluorescence emission. The S^{2-} derivative was then able to cross-link these nanoparticles to form fluorescent nanorods, which could be induced by Pb^{2+} to be converted into PbS quantum dots (QDs) in the presence of Pb^{2+}, with a significant increase in the quantum yield of the system accompanied by a significant fluorescence color change (Fig. 39b). These processes could be utilized for highly sensitive and selective fluorescence detection of S^{2-} and Pb^{2+} with LOD of 3.17×10^{-7} mol/L and 4.52×10^{-7} mol/L, respectively. Moreover, it was also a feasible way to detect Pb^{2+} in cells *in situ* by the formation of PbS QDs.

Recently, supramolecular light-harvesting systems (LHSs) based on FRET have attracted significant interest due to their great potential in photocatalysis, bioimaging and tunable photoluminescent devices [82–85]. Macrocyclic arenes possessed the ability to bind donor molecules *via* host-guest interactions and to self-assemble into SNs, which were able to load acceptor molecules. Therefore, macrocyclic arenes were widely used in the construction of supramolecular LHSs [86–88].

Yang's group developed various color-tunable SNs based on pillar[*n*]arenes [89,90]. In 2019, they attached P5 to the side chains of the polymers to obtain **37** [89]. Subsequently, they obtained supramolecular polymer networks *via* host-guest interactions be-

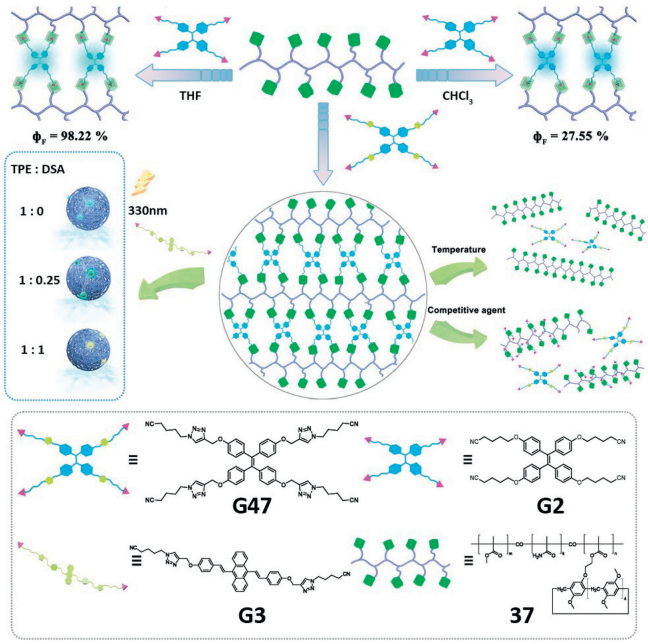

Fig. 40. Chemical structures of **37**, **G2**, **G3** and **G47**, and schematic illustrations of the construction and property study of supramolecular polymer networks. Reproduced with permission [89]. Copyright 2019, Wiley Publisher.

tween **37** and two TPE derivatives, **G47** and **G2** (Fig. 40). Furthermore, by finely adjusting the parameters, an exceptionally high fluorescence quantum yield of 98.22% was achieved for the polymers in THF. Additionally, **G3** was introduced into the polymer, leading to the formation of a series of color-tunable SNs for light-trapping systems by varying the guest ratio.

In 2020, Wang and co-workers [91,92] reported supramolecular LHSs with sequential energy transfer processes. Initially, they constructed nanoparticles through the self-assembly of host-guest complexes composed of **34** and **G48** [91]. These nanoparticles exhibited significantly enhanced fluorescence compared to free **G48**. Subsequently, they encapsulated the hydrophobic fluorescent dye Eosin Y (ESY) through non-covalent interactions, enabling energy transfer from **G44** to ESY. ESY further transferred energy to a second acceptor, Nile Red (NiR), achieving an efficient two-step energy transfer process (Fig. 41). Additionally, by adjusting the donor/acceptor ratio to 100:5:2 (**G48**/ESY/NiR), the system achieved white light emission with CIE coordinates of (0.33, 0.33).

Recently, Wang *et al.* constructed one kind of fluorescent supramolecular vesicles using a clamp-like host **38** containing two P5 units and **G2** through host-guest interactions and hydrophobic interactions [93]. The vesicles exhibited enhanced fluorescence intensity, photostability, and thermal stability. Subsequently, a LHS was developed by employing cyano-vinyl derivatives as energy donors, enabling fluorescence color modulation *via* FRET (Fig. 42). Notably, fluorescent ink based on the supramolecular vesicles was successfully prepared, demonstrating the system's potential applications in information encryption.

More recently, Sun's group [94] constructed a supramolecular LHS with red light emission in water. They first used **34** and **G49** to form yellow fluorescent nanoparticles by self-assembly in aqueous solution, which served as the energy donor. Subsequently, they encapsulated NIR as the energy acceptor through non-covalent interactions, achieving red light-emitting nanoparticles (Fig. 43) with just 1% co-assembled NiR (as low as 2×10^{-7} mol/L). These red-emitting nanomaterials were suitable for typical powder dusting approach to develop latent fingerprint patterns on various sub-

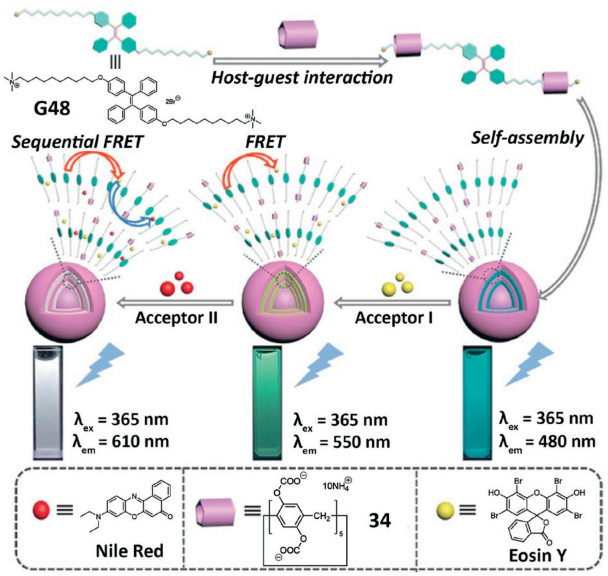

Fig. 41. Chemical structure of **G48** and schematic illustration of the self-assembly of pillar[5]arene-based LHS with two-step sequential energy transfer. Reproduced with permission [91]. Copyright 2019, Wiley Publisher.

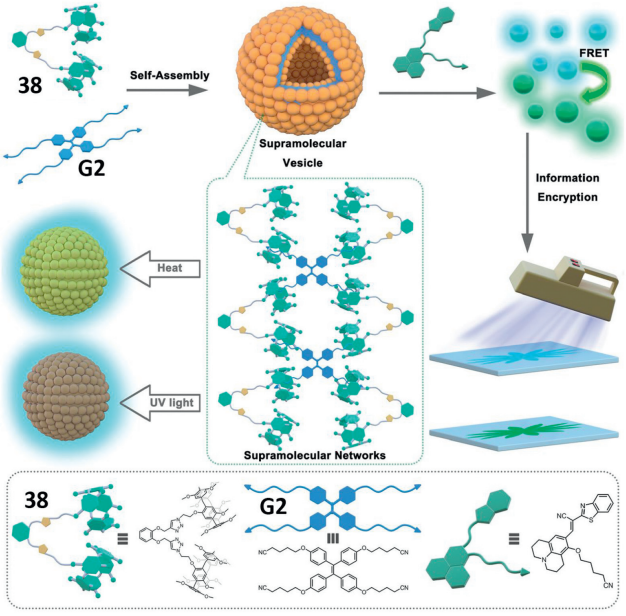

Fig. 42. Chemical structures of **38** and **G2**, and schematic illustrations of color-tunable supramolecular fluorescent vesicles with photostability and thermostability and their application in information delivery/encryption. Reproduced with permission [93]. Copyright 2022, Wiley Publisher.

strate surfaces, producing high-resolution fluorescent images and showing potential for high-contrast imaging applications.

In recent years, Liu's group had made significant contributions to the field of supramolecular ALHs [95,96]. In 2021, Liu's group developed a light-responsive supramolecular nanocomponent capable of switchable white light emission [95]. They first prepared supramolecular assemblies **G50/39[1 + 1]** and **G50/39[2 + 2]** through host-guest interactions between compound **39** and the photochromic anthracene derivative **G50**. These assemblies could further self-assemble into nanoparticles with cyan fluorescence (Fig. 44a). Next, they incorporated the energy acceptor NiR into the nanoparticles to form a supramolecular LHS. This system

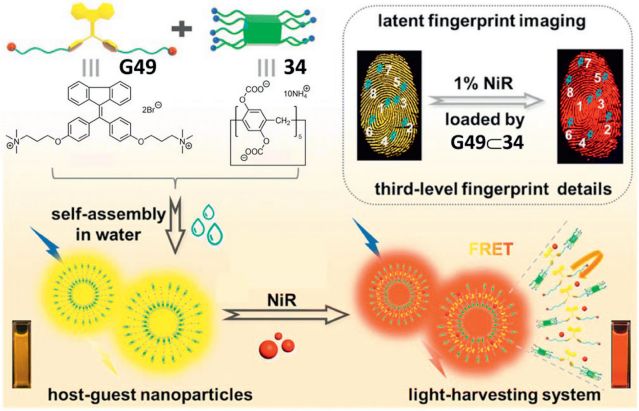

Fig. 43. Chemical structure of **G49**, and schematic illustrations of the construction of the supramolecular LHS based on **34** and **G49**, as well as its application in latent fingerprint imaging. Reproduced with permission [94]. Copyright 2023, the Royal Society of Chemistry.

exhibited a tunable photoluminescence color depending on the donor/acceptor ratio, with white light emission appearing at a CIE coordinate of (0.33, 0.34). Additionally, **G50** could switch between **G50a** and **G50b** under different light conditions, thereby reversibly blocking and restoring the resonance energy transfer (RET) between **39** and NiR (Fig. 44b). Consequently, the system could turn white light emission on or off based on the wavelength of the light (Fig. 44a). Importantly, this light-responsive supramolecular material could be used in erasable multicolor fluorescent inks for creating colored QR codes and special patterns, offering reversible hiding and revealing capabilities with significant potential for information encryption applications (Fig. 44c).

Recently, they also constructed SNs using calix[4]arene **40**, tetra-(4-pyridylphenyl)ethylene **G51**, and photoacid sulfonatomerocyanine (MEH) [97]. Within the nanoparticle, MEH could reversibly release and capture protons, while **G51** displayed pH-sensitive luminescence property. Upon irradiation at 420 nm, **G51** was converted to its positively charged form through proton transfer from the ring-closed isomer spiropyran (SP). This positively charged **G51** then assembled with the negatively charged calix[4]arene **40** *via* electrostatic interactions, forming a supramolecular assembly. The fluorescence emission of the system changed from blue to yellow and then returned to blue when the light source was removed. Furthermore, Rhodamine B (RhB) was introduced as an energy acceptor, facilitating an effective energy transfer process and resulting in the system exhibiting orange fluorescence (Fig. 45a).

Based on the light-controlled multicolor luminescence of these components, they were applied to a 3D code system. Different color blocks were used to form a color array, which could be scanned by software to read the information. As shown in Fig. 45b, the color block array was yellow in sunlight, and there was no significant difference in the luminescence color in each container under 365 nm UV light. Therefore, no information could be obtained at this time. After a 15-min exposure to 420 nm light, the fluorescent color changed, revealing Code F under UV light. This code was then scanned by software to reveal the hidden information "NKU". When the blue light exposure was removed, the fluorescent gradually returned to its original state, and the information was concealed again. Furthermore, dynamic coding was possible by adjusting the position of the color blocks. For instance, changing the position altered Code F to Code G could change the stored information from "NKU" to "C" (Fig. 45c). Code G could also respond to 420 nm irradiation, allowing for encryption of information. The dynamic transformations of the code could be repeated by irradiation and physical repositioning of the color block.

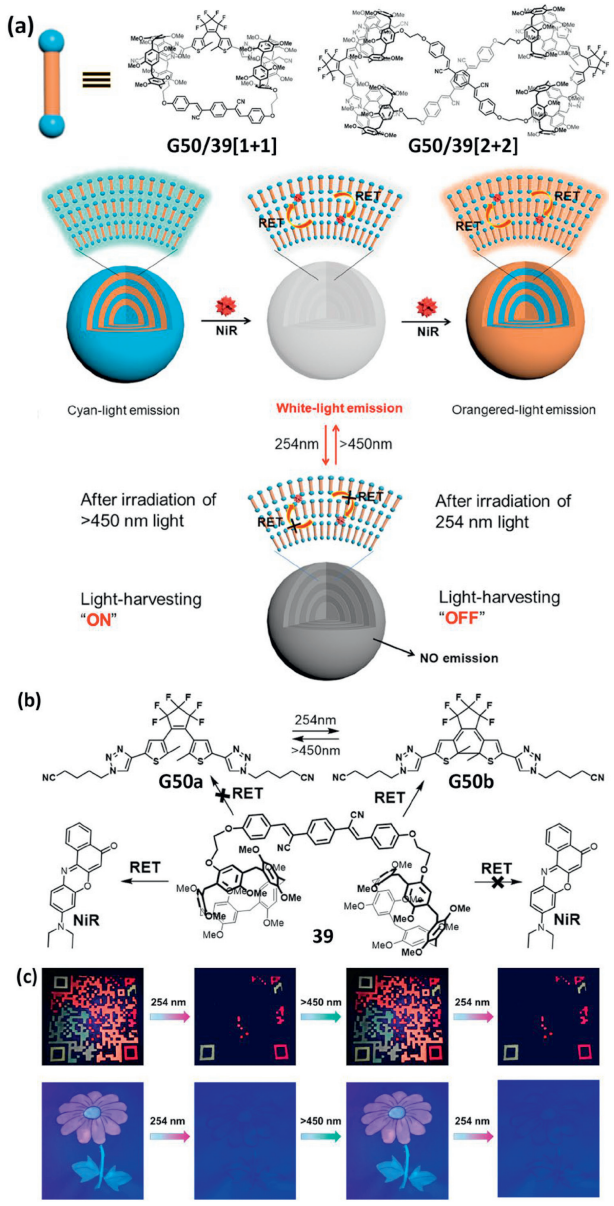

Fig. 44. (a) Chemical structures of **G50/39[1 + 1]** and **G50/39[2 + 2]** and schematic illustration of the controllable light-harvesting nanosystem based on photomodulation. (b) Schematic illustration of **G50** reversible control of energy transfer from **39** to NiR. (c) The photo-switched chromatic fluorescent QR code and photomanipulative data storage, anticounterfeiting, and data confidence. Reproduced with permission [95]. Copyright 2021, Elsevier Publishers.

Fluorescent nanoparticles based on macrocyclic arenes have been employed in biomedical applications, including bioimaging, intracellular sensing, cancer diagnosis, and drug delivery, due to their low biotoxicity and distinctive ability to recognize biomolecules. Nevertheless, the preparation process is relatively complex and their biocompatibility is yet to be deeply explored.

5. Other assemblies

The facile modification of macrocyclic arenes allows for the formation of more complex assemblies, such as nanocrystalline materials [98], metallocycles [99,100] and hybrid materials [31,101], through the synergistic effect of multiple noncovalent interactions.

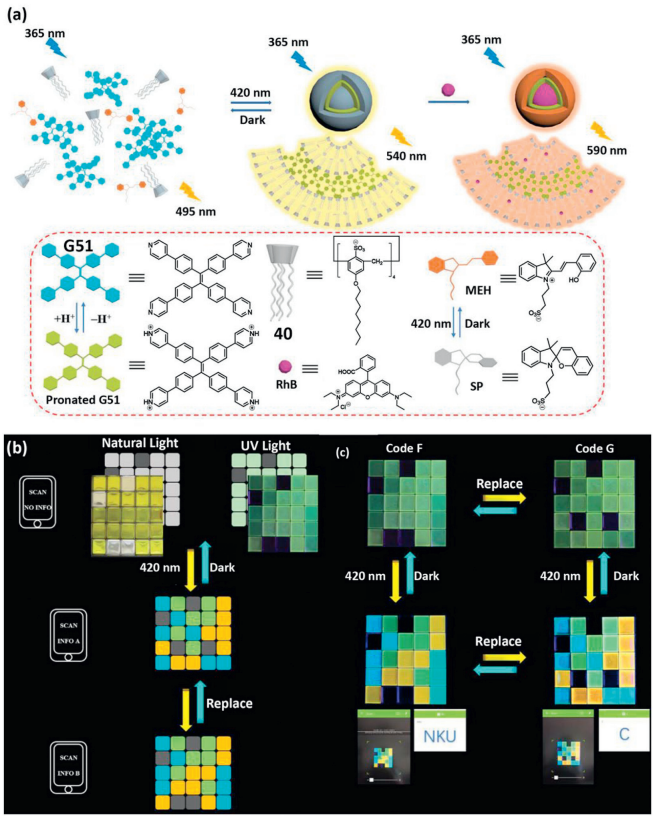

Fig. 45. (a) Chemical structures of **40** and **G51**, and schematic illustration of constructing photo-activated multicomponent supramolecular assembly. (b) Schematic illustration of the 3D code encryption. (c) Photographs of photo-responsive 3D code transformation and corresponding information. Reproduced with permission [97]. Copyright 2023, Wiley Publisher.

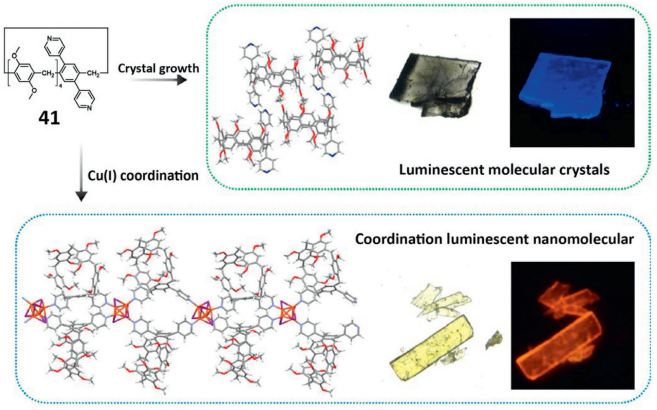

Fig. 46. Chemical structure of **41**, and the formation of luminescent molecular crystals *via* crystal growth, and coordination-driven luminescent Cu(I)–**41** nanocrystals and microscope images of **41** crystals and Cu(I)–**41** nanocrystals under sunlight and UV light (365 nm). Reproduced with permission [98]. Copyright 2021, American Chemical Society.

In 2019, Yang's group [98] prepared the luminescent molecular crystals of macrocycle **41**, and found that the crystals exhibited enhanced blue fluorescence due to the unique stacking mode of **41** in the crystal structure. Moreover, the coordination luminescent nanocrystals with significantly long luminescence lifetimes were also obtained by the coordination of **41** and Cu(I), resulting in tunable emission property (Fig. 46).

In 2020, Stang and co-workers [99,100] prepared a hexagonal Pt metallacycle **42** through the self-assembly driven by coordination interactions. The P5 in this metallacycle was able to bind **G52** through host-guest interactions, facilitating coaggregation between **G52** and P5 (Fig. 47a). This coaggregation significantly enhanced the fluorescence intensity of the system. Additionally, they constructed four triangular metallocycles (Fig. 47b) using planar chiral **43**, and found that all these metallocycles exhibited CPL property, indicating their potential applications in optical materials.

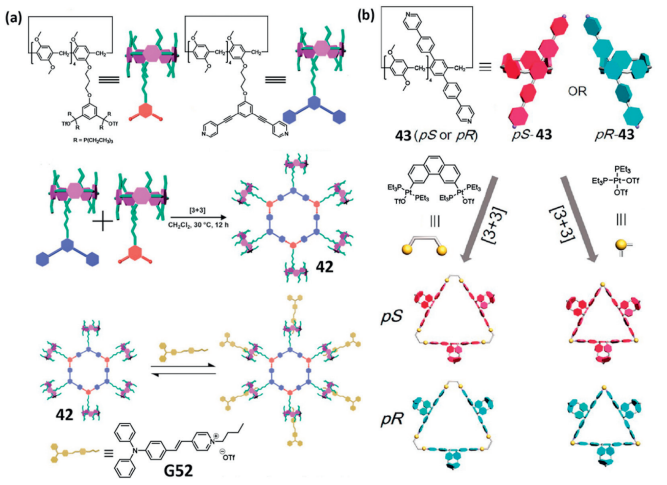

Fig. 47. (a) Synthetic route of **42**, chemical structures of **42** and **G52**, and host-guest interaction between **42** and **G52**. Reproduced with permission [99]. Copyright 2020, American Chemical Society. (b) Chemical structure of *pS*/*pR*-**43** and schematic illustration of metallacycles based on **43**. Reproduced with permission [100]. Copyright 2020, the Royal Society of Chemistry.

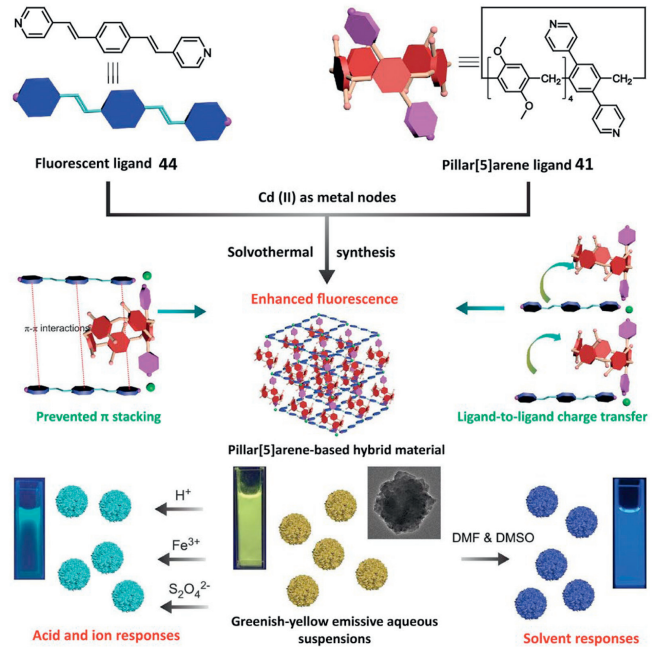

Fig. 48. Chemical structures of **41** and **44**, and schematic illustrations of the synthesis of hybrid material, the proposed fluorescence tuning mechanisms, and the tunable luminescent responses of hybrid material toward different external stimuli. Reproduced with permission [102]. Copyright 2021, Oxford University Press.

By using **41**, oligo(phenylenevinylene) (**44**) and Cd(II) metal cores, Yang's group [102] synthesized a hybrid material (Fig. 48). The hybrid material showed enhanced fluorescence emission due to the minimized π-π stacking and efficient charge transfer property benefitting from the presence of **41**. Additionally, the material displayed tunable multicolor emission in response to various external stimuli, such as solvents, ions and acid (Fig. 48). For instance,

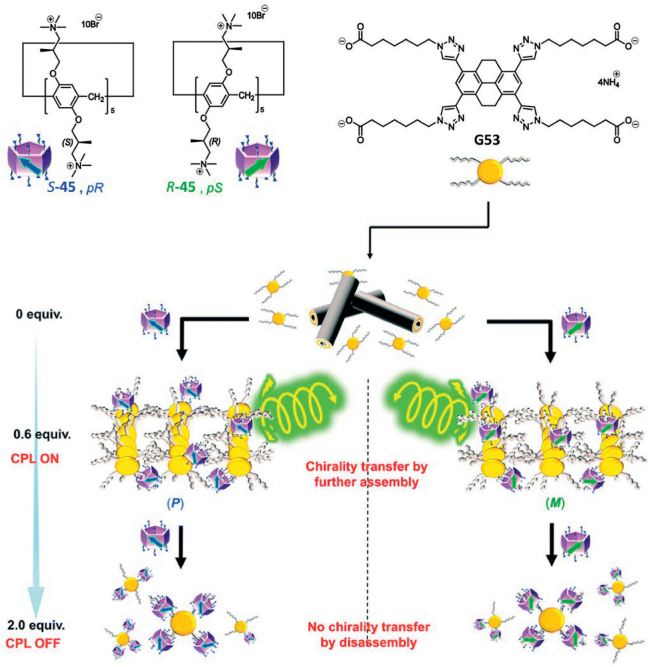

Fig. 49. Chemical structures of *S*/*R*-**45** and **G53**, and schematic illustration of new supramolecular CPL on/off controllable materials using water-soluble planar chiral pillar[5]arenes *S*-**45** and *R*-**45**. Reproduced with permission [103]. Copyright 2022, the Royal Society of Chemistry.

the hydrolyzation of Fe^{3+} ions resulted in pyridinic protonation of **44**, intercepting the charge transfer process and changing the fluorescence emission of the hybrid material from yellowish-green to cyanic.

In 2022, Ogoshi's group [103] reported a CPL on/off control system based on helical fibre assemblies. They synthesized water-soluble pillar[5]arene *S*-**45** and *R*-**45**. *S*-**45**/*R*-**45** as chiral sources, which could transfer chiral information to the assembly of a water-soluble compound **G53**, through host-guest interaction, thereby providing CPL property. Due to the large size and strong host-guest binding ability of *S*-**45**/*R*-**45**, the chiral transfer efficiency and resulting CPL property were highly sensitive to the feed ratio of the *S*-**45**/*R*-**45**. When the limited amounts (0.6 equiv.) of *S*-**45**/*R*-**45** were mixed with **G53**, they could assemble into helical fibres with CPL property. However, a large amount (2 equiv.) of *S*-**45**/*R*-**45** disrupted the helical fibres, resulting in the loss of chirality and CPL property (Fig. 49). This strategy demonstrates that the chirality of supramolecular CPL materials could be finely regulated by using macrocyclic arenes as the chiral sources.

6. Conclusion

Supramolecular luminescent materials are notable for their exceptional responsiveness to stimuli and dynamic tunability, which stem from the reversible nature of non-covalent interactions. These materials offered significant advantages over traditional luminescent materials in terms of regulating construction and photophysical properties. In recent years, a growing number of macrocyclic arenes-based SLMs have been prepared, providing a diverse range of regulatory mechanisms and photophysical properties for SLMs. The diverse applications of these macrocyclic arenes-based SLMs in various fields have also been extensively investigated. This review provided a comprehensive summary of novel SLMs based on macrocyclic arenes that have emerged in the last several years. Based on the structures of the assemblies, we highlighted the employment of supramolecular assembly strategies to fabricate luminescent materials, involving host-guest complexes, supramolecular polymers, nanoparticles, and other assemblies. Moreover, the applications of these SLMs in the fields of fluorescence sensing, information encryption, and bio-imaging were also mentioned.

Although more and more SLMs based on the macrocyclic arenes have been constructed, there are still some key points which need to be considered for improving their properties and achieving their practical applications. Firstly, the majority construction of SLMs based on macrocyclic arenes were derived from classic macrocyclic arenes, while novel macrocyclic arenes were rarely reported. However, a growing number of novel macrocyclic arenes composed of various aromatic building blocks with diverse special properties have been reported in the last several years. The construction of supramolecular luminescent materials based on novel macrocyclic arenes can bring better performance and inject fresh blood into this field. Secondly, TADF and RTP had attracted growing attention because of their unique generation processes and long-lived luminescence, which can be widely applied to the fields of optoelectronic devices, luminescence imaging, sensing, information encryption, and so on [104–108]. However, most of the SLMs based on macrocyclic arenes showed fluorescence emission. Only a few SLMs have been employed in constructing supramolecular TADF or RTP materials. Development of novel supramolecular strategy to construct TADF or RTP materials offers a new way and perspective for their practical applications in materials science. Thirdly, some macrocyclic arenes based crystalline materials exhibited excellent luminescent properties; however, they were difficult to prepare on a large scale, and they had long preparation cycle and poor operability, which significantly constrained their potential applications. Thus, it is necessary to develop other assembly forms, such as polymer materials that maintain their original luminescent property while also possessing excellent thermal stability and excellent processability. Finally, chiral macrocyclic arenes also represented a research hotspot due to their potential in the construction of CPL materials. However, the g_{lum} values of these materials were relatively low. Therefore, in order to solve these current problems and realized their potential applications, it is necessary to develop more novel macrocyclic arenes with various functions, especially those with luminescence or chirality, which are still few and far between. Furthermore, the complexation properties between the hosts and guests will be studied in detail to develop new strategies for constructing supramolecular luminescent materials. Last but not least, new assembly behaviour should be studied to improve their performance and achieve their applications.

Altogether, the study endeavour for supramolecular luminescent materials is still at the preliminary stage. There also exist many challenges and limitations for the practical applications of SLMs. For example, the synthesis steps are often lengthy and costly, and difficult to prepare on a large scale, resulting in increased application costs. Supramolecular forces including hydrogen bonding, C–H$\cdots\pi$, π-π stacking, hydrophobic effects, electrostatic effects, charge transfer interactions and so on are relatively weak compared to covalent bonds, and during the process of making devices, they are often disrupted, making it difficult to reach technical specifications. The functionality achieved through supramolecular assembly is unstable, and there may still be the issues of repeatability. However, everything has two sides, and supramolecular systems can provide good responsiveness to external stimuli, thus having great applications in the field of smart luminescent materials. We hope that this review will not only be very helpful for the development of macrocyclic arene chemistry, but also provide some valuable guidance toward the design of smart supramolecular luminescent materials.

Declaration of competing interest

The authors declare that they have no known competing financial interests or personal relationships that could have appeared to influence the work reported in this paper.

CRediT authorship contribution statement

Yu-Jie Long: Writing – original draft, Formal analysis, Data curation, Conceptualization. **Xiao-Ni Han:** Writing – review & editing, Formal analysis, Data curation. **Ying Han:** Writing – review & editing, Writing – original draft, Funding acquisition, Formal analysis, Conceptualization. **Chuan-Feng Chen:** Writing – review & editing, Supervision, Funding acquisition, Conceptualization.

Acknowledgments

We thank the National Natural Science Foundation of China (Nos. 22171272, 22031010), the Strategic Priority Research Program of the Chinese Academy of Sciences (No. XDB0520302) and the Youth Innovation Promotion Association CAS (No. 2021035) for financial support.

References

[1] J. Li, J.X. Wang, H.X. Li, et al., Chem. Soc. Rev. 49 (2020) 1144–1172.
[2] X. Hou, C. Ke, C.J. Bruns, et al., Nat. Commun. 6 (2015) 6884.
[3] H.Y. Zhou, D.W. Zhang, M. Li, C.F. Chen, Angew. Chem. Int. Ed. 61 (2022) e202117872.
[4] X.K. Ma, Y. Liu, Acc. Chem. Res. 54 (2021) 3403–3414.
[5] A.J.P. Teunissen, C. Pérez-Medina, A. Meijerink, W.J.M. Mulder, Chem. Soc. Rev. 47 (2018) 7027–7044.
[6] W.C. Geng, Z.J. Ye, Z. Zheng, et al., Angew. Chem. Int. Ed. 133 (2021) 19766–19771.
[7] X.Q. Tian. M.Z. Zuo, P.B. Niu, K.Y. Wang, X.Y. Hu, Chin. J. Org. Chem. 40 (2020) 1823.
[8] X.H. Cao, A.P. Gao, J.T. Hou, T. Yi, Coord. Chem. Rev. 434 (2021) 213792.
[9] C.X. Guo, A.C. Sedgwick, T. Hirao, J.L. Sessler, Coord. Chem. Rev. 427 (2021) 213560.
[10] X.Y. Lou, Y.W. Yang, Adv. Mater. 32 (2020) 2003263.
[11] L. Liu, T.T. Hao, W.H. Wu, C. Yang, Chin. J. Org. Chem. 43 (2023) 2189.
[12] D. Li, Z.F. Feng, Y.J. Han, et al., Adv. Sci. 9 (2022) 2104790.
[13] D.X. Ren, L. Tang, Z.Y. Wu, et al., Chin. Chem. Lett. 34 (2023) 108617.
[14] Q.Y. Feng, S.J. Zhu, B.Y. Wang, et al., Adv. Funct. Mater. 34 (2024) 2312622.
[15] C.J. Yin, Z.A. Yan, X. Ma, Chem. Commun. 59 (2023) 13421–13433.
[16] G.W. Zhang, P.F. Li, Z. Meng, et al., Angew. Chem. Int. Ed. 128 (2016) 5390–5394.
[17] C.-F. Chen, Y. Han, Acc. Chem. Res. 51 (2018) 2093–2106.
[18] J. Li, Y. Han, C.F. Chen, Chin. J. Org. Chem. 40 (2020) 3714–3737.
[19] X.N. Han, Y. Han, C.F. Chen, Chem. Soc. Rev. 52 (2023) 3265–3298.
[20] J.R. Wu, Y.W. Yang, Chem. Commun. 55 (2019) 1533–1543.
[21] S.N. Lei, H. Cong, Chin. Chem. Lett. 33 (2022) 1493–1496.
[22] H.Y. Zhou, Y. Han, Q. Shi, C.F. Chen, Eur. J. Org. Chem. (2019) 3406–3411 2019.
[23] H.Y. Zhou, Y. Han, Q. Shi, C.F. Chen, J. Org. Chem. 84 (2019) 5872–5876.
[24] T.L. Mako, J.M. Racicot, M. Levine, Chem. Rev. 119 (2019) 322–477.
[25] R. Kumar, A. Sharma, H. Singh, et al., Chem. Rev. 119 (2019) 9657–9721.
[26] D.R. Cao, H. Meier, Chin. Chem. Lett. 30 (2019) 1758–1766.
[27] J. Yang, D.H. Dai, L.J. Ma, Y.W. Yang, Chin. Chem. Lett. 32 (2021) 729–734.
[28] M.J. Gu, X.N. Han, Y. Han, C.F. Chen, ChemPlusChem 89 (2024) e202400023.
[29] K.Y. Wang, R.B. Zhang, Z.J. Song, et al., Adv. Sci. 10 (2023) 2206897.
[30] K. Velmurugan, A. Murtaza, A. Saeed, et al., CCS Chem. 4 (2022) 3426–3439.
[31] N. Song, X.Y. Lou, H. Yu, et al., Mater. Chem. Front. 4 (2020) 950–956.
[32] X. Wang, X.Y. Lou, X.Y. Jin, F. Liang, Y.W. Yang, Research 2019 (2019) 1454562.
[33] W.M. Wang, D.H. Dai, J.R. Wu, et al., Chem. Eur. J. 27 (2021) 11879–11887.
[34] X.Y. Lou, N. Song, Y.W. Yang, Chem. Eur. J. 25 (2019) 11975–11982.
[35] Y. Zhang, Z.R. Xu, T. Jiang, Y.Y. Fu, X. Ma, J. Mater. Chem. C 11 (2023) 1742–1746.
[36] Y. Guo, Y. Han, C.F. Chen, Front. Chem. 7 (2019) 543.
[37] Y. Guo, Y. Han, C.F. Chen, Molecules 27 (2022) 3932.
[38] J. Li, H.Y. Zhou, Y. Han, C.F. Chen, Angew. Chem. Int. Ed. 60 (2021) 21927–21933.
[39] W.J. Li, Q.Y. Gu, X.Q. Wang, et al., Angew. Chem. Int. Ed. 133 (2021) 9593–9601.
[40] X. Qi, W.C. Li, B.B. Shi, et al., Chin. Chem. Lett. 33 (2022) 5065–5068.
[41] T. Ogoshi, Y. Hamada, R. Sueto, et al., Cryst. Growth Des. 20 (2020) 7087–7092.
[42] N. Xue, H.Y. Zhou, Y. Han, et al., Nat. Commun. 15 (2024) 1425.
[43] Y.H. Sun, L.N. Jiang, L.J. Liu, et al., Adv. Optical Mater. 11 (2023) 2300326.
[44] M.J. Gu, X.N. Han, W. Guo, Y. Han, C.F. Chen, Angew. Chem. Int. Ed. 135 (2023) e202305214.
[45] L. Brunsveld, B.J.B. Folmer, E.W. Meijer, R.P. Sijbesma, Chem. Rev. 101 (2001) 4071–4098.
[46] P. Wang, B.C. Liang, D.Y. Xia, Inorg. Chem. 58 (2019) 2252–2256.
[47] F. Lu, Y. Yin, J. Zhao, et al., Tetrahedron 151 (2024) 133782.
[48] B. Hua, C. Zhang, W. Zhou, et al., J. Am. Chem. Soc. 142 (2020) 16557–16561.
[49] B.B. Shi, Y.P. Chai, P. Qin, et al., Chem. Asian J. 17 (2022) e202101421.
[50] Z.Q. Cao, F. Yang, D.P. Wu, et al., Polym. Chem. 14 (2023) 1318–1322.
[51] L. Shao, B. Hua, X.R. Zhao, S. Lu, G.F. Li, Chem. Eur. J. 29 (2023) e202303071.
[52] L.X. Xu, Z.Y. Wang, R.R. Wang, et al., Angew. Chem. Int. Ed. 132 (2020) 9994–9999.
[53] Y. Wu, H.Y. Qin, J. Shen, et al., Chem. Commun. 58 (2022) 581–584.
[54] J.H. Ma, Y. Han, W.C. Guo, H.Y. Lu, C.F. Chen, CCS Chem 6 (2024), doi:10.31635/ccschem.024.202404657.
[55] X.S. Li, Y.F. Li, J.R. Wu, et al., J. Mater. Chem. A 8 (2020) 3651–3657.
[56] H.W. Yan, X.J. Yin, D. Wang, T. Han, B.Z. Tang, Adv. Sci. 10 (2023) 2305149.
[57] Q. Li, Y.Z. Liu, P.R. Liu, et al., Org. Chem. Front. 7 (2020) 399–404.
[58] W.L. Zhou, X.Y. Dai, W.J. Lin, Y. Chen, Y. Liu, Chem. Sci. 14 (2023) 6457–6466.
[59] B.C. Liang, D.Y. Xia, Y.J. Cheng, Q. Zheng, P. Wang, Dalton Trans. 52 (2023) 17099–17103.
[60] D.H. Dai, Z. Li, J. Yang, et al., J. Am. Chem. Soc. 141 (2019) 4756–4763.
[61] Z.J. Liu, J.R. Wu, C.Y. Wang, et al., Chin. Chem. Lett. 30 (2019) 2299–2303.
[62] Y.F. Li, X. Wang, C.Y. Wang, Y. Wang, Y.W. Yang, Tetrahedron 149 (2023) 133718.
[63] Y.F. Li, X.Y. Lou, C.Y. Wang, et al., Chin. Chem. Lett. 34 (2023) 107877.
[64] Y.F. Li, Z. Li, Q. Lin, Y.W. Yang, Nanoscale 12 (2020) 2180–2200.
[65] Y. Guo, Y. Han, X.S. Du, C.F. Chen, ACS Appl. Polym. Mater. 4 (2022) 3473–3481.
[66] X.W. Guan, Q. Lin, Y.M. Zhang, et al., Soft Matter 15 (2019) 3241–3247.
[67] Q. Zhao, G.F. Gong, H.L. Yang, et al., Polym. Chem. 11 (2020) 5455–5462.
[68] X.W. Sun, Z.H. Wang, Y.J. Li, et al., Macromolecules 54 (2021) 373–383.
[69] Q. Lin, X.W. Guan, Y.M. Zhang, et al., ACS Sustain. Chem. Eng. 7 (2019) 14775–14784.
[70] J.X. He, Y.M. Zhang, J.P. Hu, et al., Appl. Organometal. Chem. 34 (2020) e5519.
[71] J. Liu, Y.Q. Fan, S.S. Song, et al., ACS Sustain. Chem. Eng. 7 (2019) 11999–12007.
[72] J.P. Hu, Q. Lin, H. Yao, Y.M. Zhang, T.B. Wei, Microchem. J. 194 (2023) 109312.
[73] X. Hu, F.Y. Li, S.Y. Wang, F. Xia, D.S. Ling, Adv. Healthcare Mater. 7 (2018) 1800359.
[74] L.E. Low, J.H. Wu, J. Lee, et al., J. Control Release 324 (2020) 69–103.
[75] C. Chen, X. Ni, H.W. Tian, et al., Angew. Chem. Int. Ed. 132 (2020) 10094–10098.
[76] D. Liu, J.S. Du, S.L. Qi, et al., Mater. Chem. Front. 5 (2021) 1418–1427.
[77] X.Q. Tian, M.Z. Zuo, P.B. Niu, et al., ACS Appl. Mater. Interfaces 13 (2021) 37466–37474.
[78] H. Guo, X. Yan, B. Lu, et al., J. Mater. Chem. C 8 (2020) 15622–15625.
[79] Q. Lin, Z.H. Wang, T.T. Huang, et al., J. Mater. Chem. C 9 (2021) 3863–3870.
[80] B.B. Shi, X.X. Zhao, Y.P. Chai, et al., ChemistrySelect 7 (2022) e202200757.
[81] Y.J. Li, T.T. Huang, J. Liu, et al., ACS Sustain. Chem. Eng. 10 (2022) 7907–7915.
[82] X.M. Chen, X. Chen, X.F. Hou, et al., Nanoscale Adv. 5 (2023) 1830–1852.
[83] T.X. Xiao, W.W. Zhong, L. Zhou, et al., Chin. Chem. Lett. 30 (2019) 31–36.
[84] T.X. Xiao, X.X. Li, L.L. Zhang, et al., Chin. Chem. Lett. 35 (2024) 108618.
[85] H.W. Qian, T.X. Xiao, R.B.P. Elmes, L.Y. Wang, Chin. Chem. Lett. 34 (2023) 108185.
[86] G.P. Sun, M.H. Li, L.J. Cai, et al., J. Colloid Interface Sci. 641 (2023) 803–811.
[87] X.X. Li, Z.Y. Wu, Q. Wang, et al., ChemPlusChem 88 (2023) e202300431.
[88] T.X. Xiao, H.W. Qian, X.X. Li, et al., Dyes Pigm. 215 (2023) 111289.
[89] X.H. Wang, N. Song, W. Hou, et al., Adv. Mater. 31 (2019) 1903962.
[90] X.H. Wang, X.Y. Lou, T. Lu, et al., ACS Appl. Mater. Interfaces 13 (2021) 4593–4604.
[91] M. Hao, G.P. Sun, M.Z. Zuo, et al., Angew. Chem. Int. Ed. 132 (2019) 10181–10186.
[92] G.P. Sun, W.R. Qian, J.M. Jiao, et al., J. Mater. Chem. A 8 (2020) 9590–9596.
[93] J.L. Yu, M.X. Wu, Z.Y. Xue, et al., Adv. Optical Mater. 10 (2022) 2201496.
[94] T.X. Xiao, L.L. Zhang, D.L. Chen, et al., Org. Chem. Front. 10 (2023) 3245–3251.
[95] G. Liu, H. Zhang, X. Xu, et al., Mater. Today Chem. 22 (2021) 100628.
[96] Z.X. Liu, X.H. Sun, X.Y. Dai, et al., J. Mater. Chem. C 9 (2021) 1958–1965.
[97] R. Zhang, Y. Chen, L. Chen, Y. Zhang, Y. Liu, Adv. Optical Mater. 11 (2023) 2300101.
[98] X.Y. Lou, Y.W. Yang, J. Am. Chem. Soc. 143 (2021) 11976–11981.
[99] W. Tuo, Y. Sun, S. Lu, et al., J. Am. Chem. Soc. 142 (2020) 16930–16934.
[100] H.T.Z. Zhu, Q. Li, B.B. Shi, et al., J. Am. Chem. Soc. 142 (2020) 17340–17345.
[101] X.Y. Lou, G. Zhang, M.H. Li, Y.W. Yang, Nano Lett. 23 (2023) 1961–1969.
[102] X.Y. Lou, N. Song, Y.W. Yang, Natl. Sci. Rev. 8 (2021) nwaa281.
[103] S.X. Fa, T. Tomita, K. Wada, et al., Chem. Sci. 13 (2022) 5846–5853.
[104] M. Li, C.F. Chen, Org. Chem. Front. 9 (2022) 6441–6452.
[105] Y.J. Li, P.F. Gao, Chemosensors 11 (2023) 489.
[106] G.J. Qu, Y.P. Zhang, X. Ma, Chin. Chem. Lett. 30 (2019) 1809–1814.
[107] Q.Y. Feng, S.J. Zhu, B.Y. Wang, et al., Adv. Funct. Mater. 34 (2024) 2312622.
[108] F. Fang, L. Zhu, M. Li, et al., Adv. Sci. 8 (2021) 2102970.